Results in Optics 11 (2023) 100386

Contents lists available at ScienceDirect

Results in Optics

journal homepage: www.sciencedirect.com/journal/results-in-optics

Optical fiber sensors for heart rate monitoring: A review of mechanisms and applications

Runjie He [a], Lingyu Shen [a], Zhuo Wang [a], Guoqing Wang [b], Hang Qu [c], Xuehao Hu [d], Rui Min [a,*]

[a] Center for Cognition and Neuroergonomics, State Key Laboratory of Cognitive Neuroscience and Learning, Beijing Normal University, Zhuhai 519087, China
[b] School of Microelectronics, Shenzhen Institute of Information Technology, Shenzhen 518172, China
[c] Research Center for Advanced Optics and Photoelectronics, Department of Physics, College of Science, Shantou University, Shantou 515063, China
[d] Department of Electromagnetism and Telecommunication, University of Mons, Boulevard Dolez 31, 7000 Mons, Belgium

ARTICLE INFO

Keywords:
Optical fiber sensor
Heart rate
Fiber Bragg grating
Interference modulation
Intensity modulation

ABSTRACT

As an important part of the medical health monitoring field, heart rate (HR) monitoring has become an important application field of sensing technology in recent years. Due to the flexibility, chemical inertness, and anti-electromagnetic interference, optical fiber sensor (OFS) is widely concerned and studied in the field of HR monitoring. This paper summarizes the development of recent fiber-optic HR monitoring technology, introduces the sensing principles and applications of OFS for HR monitoring, which can be divided into intensity-based, interference-based, and FBG-based. For intensity modulation, bending and polishing methods are discussed. The main types of interference-based OFS are summarized and for FBG, packaging technology and materials are mainly introduced. Finally, the discussion and conclusions are summarized.

1. Introduction

With the increasing public concern about personal health, the monitoring of vital signs, which include heart rate (HR), respiratory rate (RR), blood pressure (BP), body temperature, and other signals, is becoming more and more important (Khan et al., 2016). The vital signs monitoring system can monitor the health status and effectively detect and prevent potential diseases (Kause et al., 2004). Therefore, monitoring vital signs is an important factor in the healing process. Due to the aging of the population, the growing shortage of nursing personnel, and the control requirements for limiting medical costs, the requirements for the vital signs monitoring system are developing toward small size (Jiang et al., 2015); easy-to-use (Hao et al., 2010); low cost (Niswar et al., 2019) and dynamic monitoring (Cardona-Morrell et al., 2016), to better prevent or reduce adverse events. In recent years, many types of vital signs sensors have been developed, such as those based on electrical conduction (Suresh Kumar and Krishnamoorthi, 2021; Al-Handarish et al., 2020), magneto-impedance (Corodeanu et al., 2014; Leonhardt and Teichmann, 2018), infrared thermal imaging (Pereira et al., 2019; Cross et al., 2013), acceleration sensing (Khosrow-Khavar et al., 2015) and light intensity sensing. Vital sign monitoring can be generally divided into direct-contact, indirect-contact and non-contact type (Zawawi et al., 2013). When the monitoring sensor is directly attached to the body surface, it is called direct-contact type vital sign monitoring; when the sensor is connected to the body through other element, like cushion and mattress, it is called indirect-contact type, otherwise, it is non-contact type vital sign monitoring. Human HR monitoring plays a leading role in vital signs monitoring as an important method to investigate human health. According to the report by WHO, in 2019, 87.8 % of deaths in high-income countries (HICs) were non-communicable diseases, of which heart disease was one of the main causes (World health statistics, 2022). Meanwhile, cancer, cardiovascular disease, diabetes, and chronic respiratory diseases caused about 33.2 million deaths worldwide, an increase of 28 % over 2000 (World health statistics, 2022). Therefore, it is necessary to monitor cardiac activity to prevent and treat related diseases. The main parameter of heart activity is HR, which is the beating frequency of the heart per minute (bpm). By measuring HR and some other parameters, such as blood pressure (Huang et al., 2022) and content of atrial natriuretic peptide (Lee et al., 2020), heart activity can be effectively monitored, thus contributing to the early diagnosis of heart system diseases, such as arrhythmia (Zaza et al., 2018); cardiovascular disease (Huang et al., 2022), and atrial fibrillation (Faust et al., 2020). The HR monitoring system may also prevent and evaluate diseases in other parts, such as chronic kidney disease (Avula et al., 2020). Thus, HR monitoring has attracted the attention of research and application fields, and many

* Corresponding author.
E-mail address: rumi@doctor.upv.es (R. Min).

https://doi.org/10.1016/j.rio.2023.100386
Received 6 October 2022; Received in revised form 4 February 2023; Accepted 12 February 2023
Available online 14 February 2023

schemes have been proposed (Shoushan et al., 2021; Zhu et al., 2019; Chen et al., 2021; Chowdhury et al., 2018; Zhang et al., 2022).

Generally, the HR and signs related to cardiac activity can be obtained in the following five ways: ballistocardiograph (BCG), electrocardiograph (ECG), pulse wave (PW), phonocardiogram (PCG), and apex cardiogram (ACG), which shown in Fig. 1 (Lin et al., 2021):

BCG is a type of micro-vibration caused by human heart activities. It is a noninvasive signal, which can be collected by detecting the mechanical signal from the patient's physical contact platform. When the heart pumps blood, it hits the blood vessels, generating forces in the opposite direction of blood flow, which are then transmitted to the body's surface (Gordon, 1877). By analyzing the BCG signal, the cardiovascular system's health and synchronous information of cardiac hemodynamics can be reflected. ECG obtains cardiac activity by measuring the bioelectrical information of the heart (Asif and Drezner, 2016). When the heart contracts, it generates tiny electrical pulses, propagating through the myocardium. ECG can be obtained by monitoring these bioelectrical pulses. PW measurement method is to roughly estimate the HR by detecting the pulse times of the large arteries, such as the radial artery and the carotid artery. In general, HR can be estimated from the pulse (Boutouyrie et al., 1999). This method is simple and convenient, but if the patient has an arrhythmia, the measured pulse number will be different from the HR. PCG measures mechanical vibration caused by myocardial contraction, valve opening and closing, blood acceleration, and other factors in the cardiac cycle. Compared with ECG, PCG can measure more heartbeat information, such as the third heart sound(S3), which reflects rapid left ventricular distention along with an increased atrioventricular flow (Shono et al., 2019), shown in Fig. 1, but because the larger sequence of heart sounds is weak, it needs filtering and amplification to obtain the signal, resulting in a more complex processing procedure. ACG is the recording of movements of the chest wall over the apex of the heart (Tippit and Benchimol, 1967). Apex pulsation will cause chest wall movement. Therefore, the pressure sensor placed on the chest can measure the apex beat to obtain an HR signal.

ECG is the most mature and widely used clinical device. It has the characteristics of high accuracy and low noise, but for the traditional ECG device for medical monitoring, like Nalong RAGE-12L (RAGE-12-Nalong health, 2023); the sensing electrode close to the skin surface is prone to fall off. Therefore, it is not suitable for daily HR dynamic monitoring. PCG can analyze multiple signs of cardiac activity but it requires complex data processing (Ghosh et al., 2020). Moreover, since the PCG signal is weak (Lin et al., 2021); additional signal amplification device, like audio amplifier module, is required (Mohamadou et al., 2022). PW is a simple and straightforward way to access HR. However, pulse and HR are not always consistent, so measuring pulse may lead to misdiagnosis. BCG is non noninvasive and can measure the body movement caused by blood injection in each cardiac cycle. Traditional BCG sensors included acceleration sensor (Khosrow-Khavar et al., 2015), piezoelectric sensor (Wang et al., 2003; Alametsä et al., 2009) and so on. It is convenient and can be used as a direct or an indirect contact device. However, electronic sensors are sensitive to electromagnetic interference, which is inapplicable in some environments, such as magnetic resonance imaging (MRI). At the same time, the BCG signal is weak and easily submerged by noise. ACG is also limited by weak signal (Lin et al., 2021). Based on the limitations of traditional HR sensors, the current research direction is toward high accuracy, simplicity, suitable for various environments, and safety. HR monitoring settings based on optical fiber sensors (OFS) have been proposed to overcome these limitations.

OFS is a modulator that converts the measured parameters into modulated optical signals. According to the modulated property, OFSs are classified into intensity modulation, phase modulation, wavelength modulation, and polarization modulation. In recent years, OFS has attracted wide attention because of its high sensitivity, strong stability, small size, and chemical inertness (Lyu et al., 2022; Samartkit and Pullteap, 2019). Compared with traditional electrical sensors, OFSs have the advantages of flexibility, anti-electromagnetic interference (anti-EMI), and high humidity resistance. With these advantages, OFSs have made progress in many fields, such as shape sensing (Amanzadeh et al., 2018), biological detection (Perri et al., 2021), liquid level sensing (He et al., 2022; Ge et al., 2020), bridge displacement measurement (Tang et al., 2020), environmental protection (Min et al., 2021), spacecraft application (Friebele et al., 2004) and human vital signs monitoring

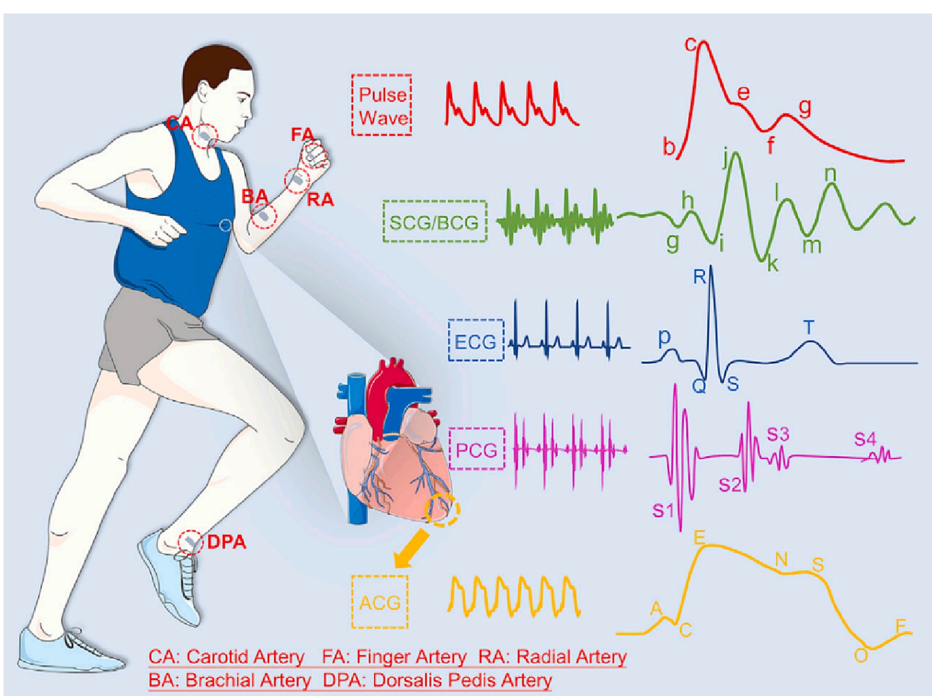

Fig. 1. Five Cardiac Activity Monitoring Methods (Chowdhury et al., 2018).

(Perezcampos Mayoral et al., 2021; Fajkus et al., 2019). In the application of OFS, as the main parameter of vital signs monitoring, HR sensor has received much attention and many types of OFSs have been proposed in the HR monitoring field. In particular, the anti-EMI characteristics of OFS makes it have potential application value in some specific environments, such as HR monitoring in MRI, while the ECG systems is inapplicable or characterized by a high price tag (Dabaghyan et al., 2016). The majority of types of optical fiber HR sensors are intensity-based, interference-based, specklegram-based and FBG-based. These different sensing types are used according to different requirements to achieve better performance. Because HR is significantly higher than RR, a non-contact method is generally not suitable for measuring HR (Zawawi et al., 2013). In the current optical fiber HR sensor, most of the indirect-contact type is based on BCG. For example, in 2019, Zhang et al. incorporated optical fibers into textiles to create intelligent mattresses. The mattresses can monitor the RR and HR of newborns during clinical trials at a periodic time (Zhang et al., 2019). This type of sensor is low-cost, flexible, and suitable for long-term monitoring. The direct-contact type is mainly measured based on ACG or PW. Using the flexibility of the optical fiber, especially polymer optical fiber (POF) (Wang et al., 2021; Teng et al., 2022), the sensing part can be close to the surface of the human body, to achieve better measurement results. For example, in 2019, Arifin et al. fabricated a POF-based sensor to detect the heart, the change of the output voltage to heartbeat over a certain period of time was tested, and the sensor sensitivity, which is defined as the division of output difference and time measurement, can reach 2.31 mV/s (Arifin et al., 2019). Moreover, FBG can inscribed in the POF (Jiang et al., 2022; Broadway et al., 2019); which can be implemented in several methods, such as femtosecond laser direct writing technique (Stefani et al., 2012) and phase mask technique (Hu et al., 2017), and has more outstanding characteristics compared with commercial silica FBG. In recent years, with the progress of optical fiber fabrication technology, this type of sensor has been greatly developed.

At present, there are relevant reports on the review of human vital signs based on OFS. For example, Mayoral et al. introduced the application of optical fiber vital sign sensors in 2021 (Min et al., 2022). Min et al. introduced the mechanisms, materials, and applications of polymer optical fiber vital sign sensors in 2022 (Leal-Junior et al., 2020). These reviews have all introduced the part about optical fiber HR monitoring, but they are limited in length and are not specific and detailed enough. Therefore, this review summarizes the development of fiber-optic HR monitoring technology in recent years, which is helpful for researchers interested in relevant fields. The first part of this paper introduces vital signs monitoring, HR monitoring, and the current development of OFS in HR monitoring. The second part introduces the principle of OFS for HR monitoring. The third part introduces the research findings in recent years, which can be divided into intensity-based, interference-based, specklegram-based and FBG-based according to the sensing technologies. Finally, the discussion and conclusions are summarized.

2. Principles

The majority types of optical fiber HR sensors are intensity-based, interference-based, specklegram-based and FBG-based. For intensity-based optical fiber HR sensors, to improve the accuracy of HR monitoring, it is usually necessary to process the optical fiber, usually bending or polishing. The interference-based optical fiber HR sensor is mainly realized by MZI or FPI. In specklegram-based optical fiber sensor, also called fiber specklegram sensor (FSS), the specklegram is excited by the mode interference of coherent light source in the multi-mode fiber (MMF), and is therefore correlated with structural deformations on the fiber (Choi et al., 2014). FBG is a kind of wavelength modulation, and the reflected wavelength is affected by the parameters to be measured. Here we introduce these OFSs structures and sensing mechanisms commonly used in HR measurement.

2.1. Intensity-based sensor

Due to the advantages of low cost and ease of fabrication, intensity-based OFS is the most widely used (Tian et al., 2017). The modulation of intensity is mainly based on the excess propagation loss. In the optical fiber HR sensor, the change of propagation loss mainly comes from the strain and bending brought by the heartbeat to the optical fiber sensing part. To improve the sensitivity, some processing of optical fiber is required, usually bending or polishing.

The principle of bent and polished loss-based OFS can be described through total internal reflection (TIR). According to Maxwell's equation, even if the light in the optical fiber meets the TIR condition, there is still a field in the low effective index cladding. It is a rapidly decaying electromagnetic wave, called an evanescent wave (EW). The strength of an evanescent wave in a low effective index medium can be expressed as:

$$E_{EW} = E_0 \bullet e^{-\frac{z}{d_p}} \tag{1}$$

where E_{EW} is the evanescent field strength, E_0 is the initial field strength, z is the distance to the reflection interface, and d_p is the penetration. d_p can be expressed as:

$$d_p = \frac{\lambda}{2\pi\sqrt{{n_1}^2 sin^2\theta_l - {n_2}^2}} \tag{2}$$

where θ_l is the incident angle. When the thickness of the optical fiber cladding is less than d_p, part of the evanescent field energy can pass through the cladding and come into contact with the substance to be measured to cause energy absorption, resulting in an additional optical loss. Thus, by polishing the cladding or even part of the core, shown in Fig. 2, excess propagation loss will be excited. Therefore, external information can be detected by measuring the intensity.

The principle of bending loss is that after bending the optical fiber, the θ_l decreases so the d_p increases. Therefore, the extra propagation loss will be produced. For bending loss, it can be divided into micro-bend and macro-bend (He et al., 2022). For micro-bend OFS, the optical fiber is limited to bending in a regular pattern, usually placed in a toothed deformer, as shown in Fig. 3 (a). When the measured parameters (such as strain, pressure, and acceleration) act on the deformer mechanically, the optical fiber will be micro-bend deformed. For the macro-bend OFS, the fiber is bent to form a shape, such as a U-shaped, shown in Fig. 3 (b), with a relatively large diameter (usually about a few centimeters). And then the bent fiber is placed on an elastic element to form an OFS. When the elastic element is deformed, the excess propagation loss will change with the change of the bending radius of the optical fiber.

2.2. Interference-based sensor

The phase difference can modify the intensity of the interference resultant wave. During measurement, measured parameters alter the light phase. The phase difference can be converted into a variation in light intensity or wavelength via interferometry. The interference-based

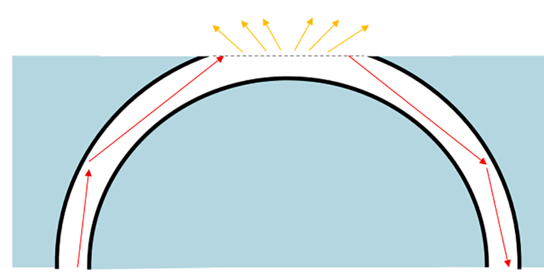

Fig. 2. Schematic diagram of optical fiber polishing loss.

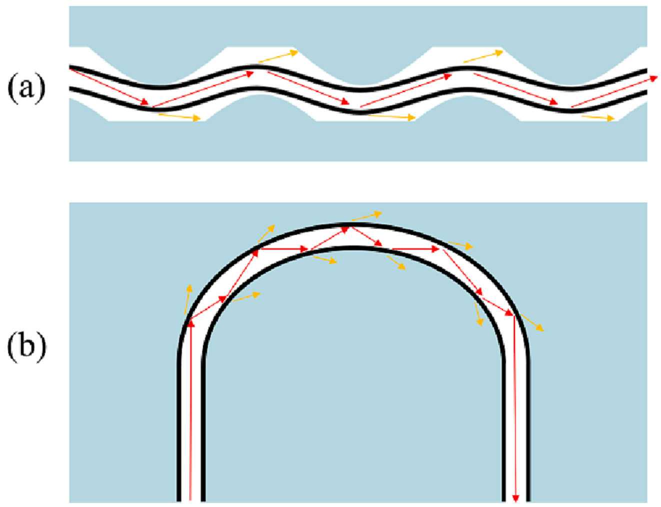

Fig. 3. Schematic diagram of optical fiber: (a) micro-bend loss and (b) macro-bend loss.

OFS has the advantages of high sensitivity and low production cost (Zhu et al., 2012).

The usual optical fiber multiple-beam interference sensor can be divided into Mach-Zehnder interferometer(MZI), Fabry-Perot interferometer(FPI), Sagnac interferometer, and Michelson interferometer (Hayashi et al., 1998). In the optical fiber HR sensor based on phase modulation, the main types used are MZI and FPI, Sagnac interferometer also has relevant studies (Lyu et al., 2022).

2.2.1. MZI-based

The optical fiber-based MZI consists of a reference arm and a sensing arm, as shown in Fig. 4. After being transmitted to the coupler, the incident light beam is propagated into both two arms. The optical length of the sensing arm, which are influenced by external parameters, determine the phase of the light in the sensing arm. Finally, the beams in the two arms are re-coupled through another coupler, and a tunable interferogram is generated due to the variable phase difference. Assume that the light intensity emitted from the reference arm is I_1, the light intensity emitted from the sensing arm is I_2, and the phase difference between the two beams is ϕ, then the output light intensity after re-coupling can be expressed as:

$$I = I_1 + I_2 + 2\sqrt{I_1 I_2}cos\phi \tag{3}$$

2.2.2. FPI-based

The cavity of an FPI is made up of two separated parallel reflecting surfaces, shown in Fig. 5. When light is transmitted into the reflecting surface, a small amount of the input light (reference signal) is reflected internally at the first reflecting surface, while the rest of the light (sensing signal) is transmitted to the FP cavity and incident on the second reflecting surface. The interference happens due to the multiple superpositions of the reference signal and sensing signal of light in these parallel surfaces. The intensity (I_r) of the resulting interference signal is subsequently detected by a photodetector and can be mathematically described by:

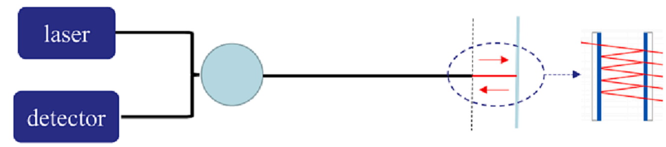

Fig. 5. Schematic diagram of optical fiber FPI.

$$I = I_1 + I_2 + 2\sqrt{I_1 I_2}\cos(\frac{4\pi\Delta L}{\lambda}) \tag{4}$$

where I_1 and I_2 are the reflection intensity of the reference signal and sensing signal; L is the initial length of the FPI; λ is the free space wavelength, and $\phi = \frac{4\pi\Delta L}{\lambda}$ is the phase difference of the two interference lights.

2.2.3. Sagnac interferometer-based

Generally, this type of interferometer uses a single fiber as the loop structure, showed in Fig. 6(a), A beam of light enters the coupler and is divided into two coherent beams. These two beams of light propagate along the loop in opposite directions to form a closed optical path, which is re-coupled on the coupler and sent to the photodetector. In this interferometer, the optical path length of the two beams is equal. When the loop of beam propagation is disturbed, Because the two optical paths are disturbed at different times, the optical path difference between the two beams will occur, resulting in interference. However, the typical Sagnac loop has poor SNR for signals generated by slight vibration, and is not sensitive to low-frequency signals, so it is difficult to detect breath and heartbeat signals. To solve these problems, one method is to connect two different types of optical fibers and place them to make the Sagnac loop in an unbalanced state, called unbalanced Sagnac loop, showed in Fig. 6(b). This unbalanced structure will cause the phase difference between the two beams even if they are not disturbed and the phase change is more like to emerge. Therefore, the unbalanced Sagnac loop is sensitive to small vibration and suitable for detecting vital signs such as HR and RR.

2.2.4. Optical fiber inter mode interference-based

The analysis methods of inter-mode interference mainly include the mode expansion propagation method and beam propagation method (BPM) (Sun et al., 2015). In the optical fiber, light in optical fiber is

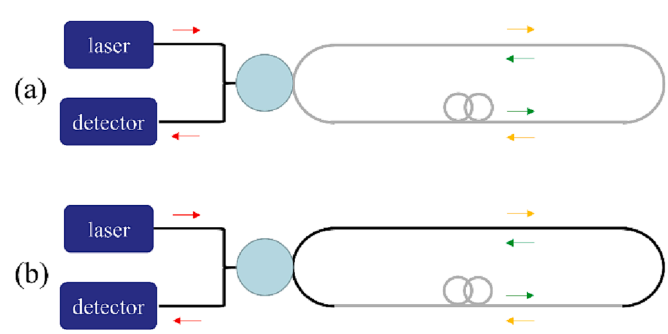

Fig. 6. Schematic diagram of (a) optical fiber FPI Sagnac loop and (b) unbalanced optical fiber FPI Sagnac loop.

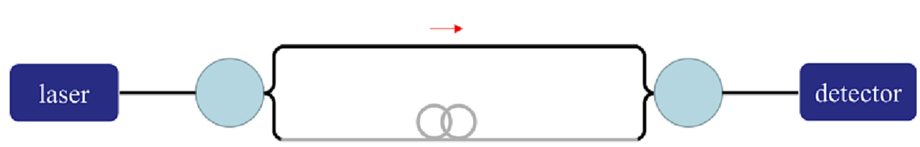

Fig. 4. Schematic diagram of optical fiber MZI.

transmitted in the form of TIR and different modes in the optical fiber have different longitudinal propagation constants β along the fiber axis:

$$\beta = \frac{2\pi n}{\lambda} \tag{5}$$

where λ Is the wavelength, n is the effective index of the optical fiber mode, which is between the core effective index n_1 and cladding effective index n_2. For the mode expansion propagation method, when light propagates in optical fiber, the modes of light are independent of each other, but in reality, propagation constants β of different modes are different, thus, the modes will produce phase differences, resulting in the redistribution of light field energy, which is called inter mode interference. Optical fiber inter-mode interference can also be considered an in-fiber MZI (Wang et al., 2021). In optical fiber interference sensors, the most typical example is the single-multi-single (SMS) structure (Guzmán-Sepúlveda et al., 2021). In this structure, light is coupled into MMF through single-mode fiber (SMF), which excites the propagation of a large number of modes in MMF. These modes interfere with each other and the energy in the fundamental mode E is decomposed and coupled to N modes of the MMF, which can be described as:

$$E(r) = \sum_{m=1}^{N} \alpha_m E_m(r) \tag{6}$$

where E is the electric field distribution, α_m is the coupling coefficient, N is the total number of modes. In the transmission process, the modes transmitting in MMF interfere with each other causing the energy redistributed (Osório et al., 2021). After the transmission in MMF, the electric field distribution after multi-mode interference (MMI) can be expressed as:

$$E(r) = \sum_{m=1}^{N} \alpha_m E_m(r) e^{i\beta_m L} \tag{7}$$

where β_m is the longitudinal propagation constant in the MMF, $E(r)$ and $E_m(r)$ are the electric field distribution of the LP_{01} mode in the SMF and LP_{0m} modes in the MMF, respectively, m is an integer number and L is transmitting length of MMF. According to formula (7), the electric field intensity E is determined by the phase difference between modes and the excitation conditions. Then the intensity after modal interference can be expressed as:

$$I(r) = E(r)E^*(r) = \sum_{m=1}^{N} \sum_{n=1}^{N} \alpha_m \alpha_n^* E_m(r) E_n^*(r) e^{i(\beta_m - \beta_n)L} \tag{8}$$

After coupling through the output SMF, the light intensity output is obtained. Fig. 7 shows a typical optical field intensity evolution of the SMF-MMF-SMF structure.

2.3. Specklegram-based sensor

In FSS, the specklegram, is generated and observed in the fiber end facet (Choi et al., 2014) and the sensing sensitivity of a FSS is mainly depends on the numbers of its speckle dots and the contrast (Rodríguez-Cuevas et al., 2017). In a step index MMF, the approximate value of the mode number (N) is given by:

$$N = \frac{V^2}{2} \tag{9}$$

where V is the normalized frequency of the MMF and can be described as:

$$V = \frac{2a\pi}{\lambda} \sqrt{{n_1}^2 - {n_2}^2} \tag{10}$$

where a is the core radius of MMF. N will determine the number of speckle particles in the specklegram, and further affect the sensing sensitivity. The distribution of speckle dots in the speckle pattern is affected by external disturbance. Due to the spatial randomness of the distribution, probability and statistics are required to described the speckle pattern. The intensity of each individual speckle may vary, while the total intensity of the speckle pattern remains constant (Efendioglu, 2017). To achieve the HR monitoring, typically the normalized intensity inner product (NIPC) method is used, which is given as:

$$NIPC(t) = \frac{\iint I_0 I(t) dS}{\sqrt{\iint {I_0}^2 dS \iint I^2(t) dS}} \tag{11}$$

where I_0 is the original intensity of a pixel in a speckle pattern and $I(t)$ is the intensity of a pixel under the disturbance. Thus, the sensitivity of FSS is also affected by the resolution of imaging devices, generally charged coupled device (CCD) (Wang et al., 2021). Fig. 8 shows a typical MMF speckle pattern.

2.4. FBG-based sensor

Fiber Bragg grating (FBG) is a micro resonant structure that is fabricated by manufacturing the periodic change of the optical fiber core RI, this periodic structure reflects a narrow spectral band of light and the center wavelength of the reflected spectrum is called Bragg wavelength

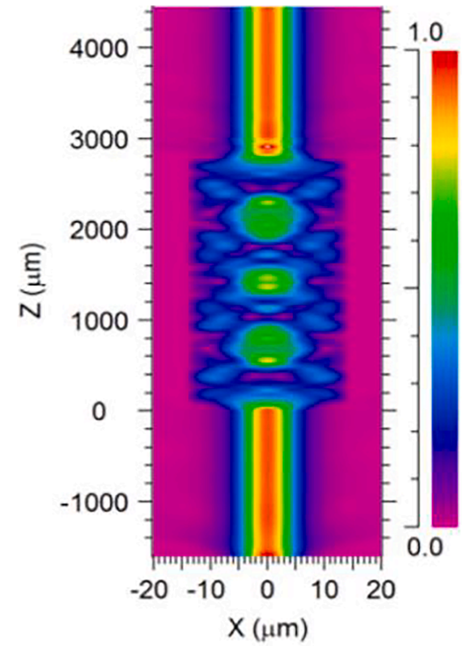

Fig. 7. A typical optical field intensity evolution along the SMF-MMF-SMF length (z-axis) (Benevides et al., 2015).

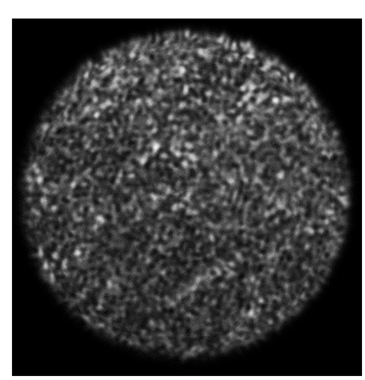

Fig. 8. A typical MMF speckle.

λ_B, which can be described as:

$$\lambda_B = 2n_{eff}\Lambda \tag{12}$$

where Λ is the grating period and n_{eff} is the effective index of the optical fiber core. When external information changes Λ and n_{eff}, the change of external information can be detected, shown in Fig. 9. For FBG, the parameters Λ and n_{eff} of Bragg wavelength λ_B are greatly affected by strain and temperature. If it is considered that other effects can be ignored, λ_B can be considered as a function of strain and temperature $\lambda_B(\varepsilon, T)$. Therefore, the wavelength shift $\Delta\lambda_B$ can be expressed as:

$$\Delta\lambda_B = 2\left(\Lambda\frac{\partial n_{eff}}{\partial \varepsilon} + n_{eff}\frac{\partial \Lambda}{\partial \varepsilon}\right)\Delta\varepsilon + 2\left(\Lambda\frac{\partial n_{eff}}{\partial T} + n_{eff}\frac{\partial \Lambda}{\partial T}\right)\Delta T = S_\varepsilon\Delta\varepsilon + S_T\Delta T \tag{13}$$

where S_ε and S_ε are the strain-sensitive constant and temperature-sensitive constant.

3. HR monitoring applications

In HR monitoring applications, intensity modulation is the most easily realized optical fiber sensor modulation. However, the low signal-to-noise ratio (SNR) and ease of interference with intensity-based OFS must be considered. Therefore, additional operations to optical fiber such as bending or polishing (Zhao et al., 2021) are usually required to increase the sensitivity to strain. Other methods, such as adopting specific filtering algorithms to extract relatively weak HR signals from the spectrum (Wang et al., 2020), can also improve SNR. The main types of interference-based OFS for HR monitoring are MZI and FPI, which have high sensitivity, simple fabrication, or compactness but a complex demodulated system is required when phase modulation is adopted (Nedoma et al., 2018; Leal-Junior et al., 2019). For FSS, the receiver only needs to use a camera, so the FSS system is cost-efficient, especially compared with the FBG-based sensing system. FBG is mainly used for BCG in HR monitoring. Its accuracy is the highest among the four sensing technologies, meanwhile its cost is also the highest among them. FBG is applied to direct-contact type devices and encapsulation is generally used to make up for the relatively fragile disadvantage of FBG. Intensity-based, interference-based, specklegram-based and FBG-based sensing technologies each have distinctive features regarding cost, complexity, and accuracy. Table 1 shows the characteristics comparison of optical fiber HR sensor based on these sensing technologies, and for each technology mentioned, a typical work of nearly-three years has been selected as the basis for comparison of performance.

Table 1
Performance comparison of optical fiber HR sensor based on different sensing technologies.

Ref.	Technology	Cost	Complexity	Accuracy
(Zhan et al., 2020)	Intensity-based	Low	Low	Low
(Nedoma et al., 2018)	Interference-based	Medium	Medium	Medium
(Tavares et al., 2022)	Specklegram-based	Low	Medium	Low
(Kuang et al., 2022)	FBG-based	High	High	High

3.1. HR monitoring based on OFS with intensity modulation

The optical fiber HR sensor based on light intensity modulation is usually realized based on the direct correlation between the intensity attenuation in the optical fiber and the body movement (mainly the chest) caused by the heartbeat. Since the movement caused by respiration is larger than the heartbeat, usually the HR sensor can be used to monitor RR at the same time to increase the usability of the sensor (Koyama et al., 2018). This method of directly using optical fiber as a sensing device is simple, but the SNR of this method is low and it is easy to be interfered by other factors (such as other body movements) (Suaste-Gómez et al., 2014). Therefore, additional operations are usually required to increase the sensitivity of the optical fiber to strain, such as bending or polishing the optical fiber (Zhao et al., 2021), or adopting specific filtering algorithms to extract relatively weak HR signals from the spectrum. For example, a filtering algorithm is adopted to extract the HR and RR signals from the original signals of the sensor (Wang et al., 2020). Table 2 and Fig. 10 describes the recent intensity-based optical fiber HR sensors.

The most direct application of the optical fiber HR sensor is to put the sensing part on the chest or wrist for measurement. Leal junior et al. proposed a POF-based HR sensor and related algorithms in 2019 (Zhan et al., 2020). The softness of POF can make it cling to the chest and be bent and polished at multiple ends to increase the sensitivity, shown in Fig. 11 (a). Moreover, the frequency and amplitude of the measured signal are analyzed to reduce noise interference. Subjects were asked to be seated or walk for 30 s. The results show that the sensor can monitor HR and RR effectively even if the subject performs periodic body movements caused by gait. There are also indirect-contact measurement methods, which increase the area of the sensing part by integrating the sensing part into the mattress or cushion. For example, Zhang et al. designed an OFS with toothed deformer mesh micro-benders to simultaneously monitor the infant's perioperative HR and RR in 2019 (Zhang et al., 2019), shown in Fig. 11 (b). The sensor was embedded into the operating bed and tested for 10 perioperative infants. The results show that the proposed OFS has good consistency with the standard

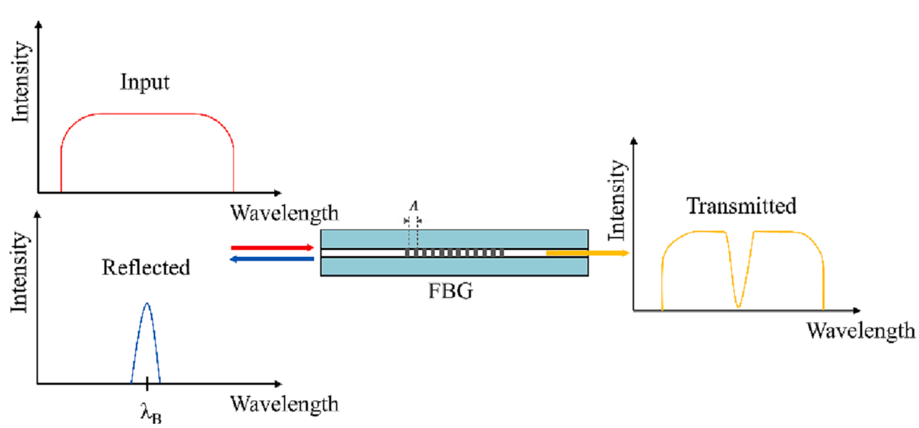

Fig. 9. Schematic diagram of FBG. (Red) input light spectrum, (Blue) reflected spectrum and (Yellow) transmitted spectrum. (For interpretation of the references to colour in this figure legend, the reader is referred to the web version of this article.)

Table 2
Intensity-based optical fiber HR sensors

Type	Material	Structure	Mean absolute error for RR	Mean absolute error for HR	Year	Ref.
Direct-contact	PMMA-POF	• Unmodified • Macro-bending	-	-	2014	(Chen et al., 2014)
	No-jacket POF (980 μm cladding)	• Coiled	-	-	2019	(Arifin et al., 2019)
	PMMA-POF (HFBR-EUS100Z)	• Polished • Macro-bending	0.7 rpm (seated) 1 rpm (walk)	2.9 bpm (seated) 4 bpm (walk)	2019	(Zhan et al., 2020)
Indirect-contact	GI-MMF (100/125)	• Serpentine array • Micro-bending	1.7 rpm	1.2 bpm	2014	(Wang et al., 2021)
	GI-MMF (100/125)	• Serpentine array • Micro-bending	1.0521 rpm	1.5594 bpm	20192021	(Zhang et al., 2019; Han et al., 2021)
	POF (980 μm cladding)	• Polished • Long ring shape	0.7 rpm	1.7bpm	2021	(Wang et al., 2022)
	GI-MMF (YOFC 100/125)	• Dual fiber path • Micro-bending	1.02 rpm	3.60 bpm	2022	(Li et al., 2022)

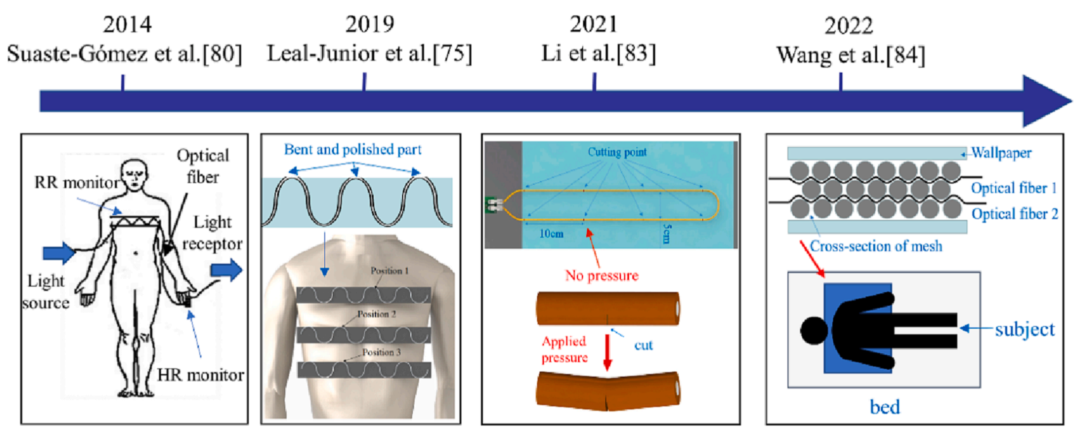

Fig. 10. Some intensity-based HR OFS reported in recent years.

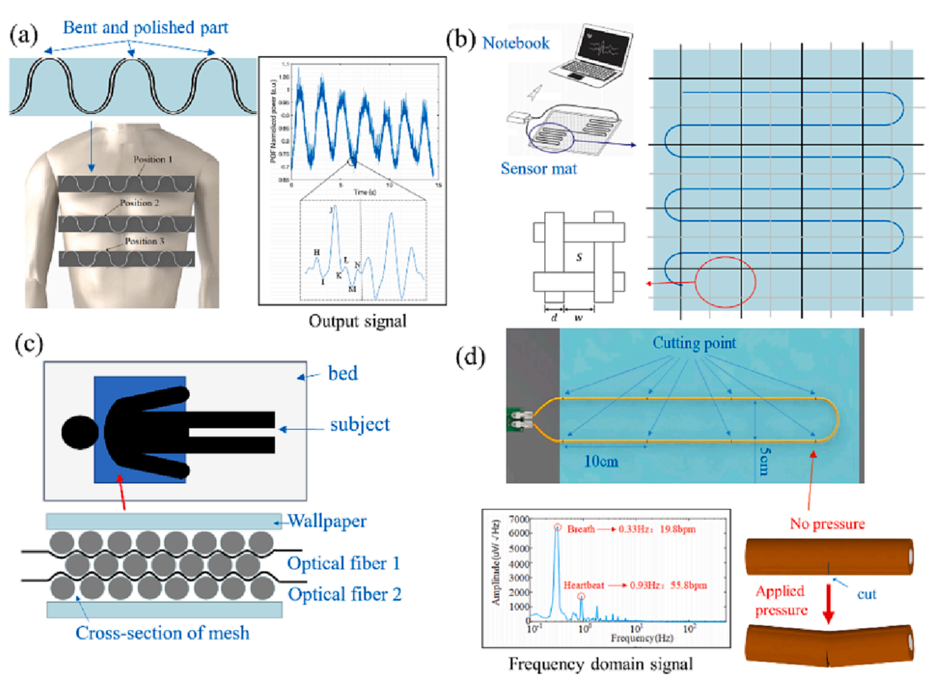

Fig. 11. Intensity-based optical fiber HR sensor and their output signals: (a) direct-contact type based on bent and polished POF (Zhan et al., 2020), (b) mesh micro benders mattress (Zhang et al., 2019), (c) dual-path micro-bend structure (Li et al., 2022), and (d) polished POF-based matrix (Wang et al., 2022).

monitoring in the absence of gross movement and a non-active resting state. Furthermore, in 2021, based on the above work presented by Zhang in 2019, a deep learning model was proposed to process HR and RR information. The experimental results show that the deep learning model has a better effect than the traditional FFT algorithm and WT algorithm (Han et al., 2021). Wang et al. designed a novel dual-path micro-bend fiber sensor for non-invasive monitoring of RR and HR of cancer patients and the false report rate, which the ratio of wrong data (data with large difference between measured value and reference value) to all measured data, is reduced by comparing the data of dual-path optical fibers in 2022 (Li et al., 2022), shown in Fig. 11 (c). By comparing the data of two-path fiber, a part of the wrong data is eliminated to reduce the error reporting rate of HR and RR. For the monitoring of cancer patients, patients are required to lie on the mattress with integrated sensors, and the false report rate of dual-path micro-bend fiber sensors was 12.87 %, which was smaller than that of single-path fiber sensors (19.09 %). Han et al. proposed an intelligent matrix based on a POF sensor to monitor human RR and HR, in which POF is partially cut to achieve additional loss, thereby increasing the sensitivity to RR and HR in 2021 (Wang et al., 2022), shown in Fig. 11 (d). During the experiments, subjects were asked to lie on the mattress for 30 s and one of them were required to lie in a supine, left, right or prone posture for 30 s respectively. Results show that the sensor can distinguish four different sleeping positions and monitor the RR and HR under different positions. The absolute errors of RR and HR are less than 1 bpm and 2 bpm respectively. In general, low cost and easy fabrication are the main advantages of intensity modulation optical fiber HR sensors, so there are many studies on this type of sensor.

3.2. HR monitoring based on OFS with interference

In the interference-based optical fiber HR sensor, the main types used are MZI and FPI because they fit the transmission characteristics and methods of optical fiber. This kind of OFS has high sensitivity but complex demodulated system is required when phase modulation is adopted, which limit its cost. (Zhu et al., 2012; Li et al., 2019). In the optical fiber HR sensor, the main types used are MZI and FPI because they fit the transmission characteristics and methods of optical fiber (Lyu et al., 2022). Table 3 and Fig. 12 describes the recent interference-based optical fiber HR sensors.

3.2.1. OFS with MZI for HR monitoring

MZI is characterized by no reflection, high utilization of light source, and strong interference effect. However, the complex package and high symmetry requirement of both arms led to the signal fading effect, which will affect HR monitoring performance (Knudsen and Bløtekjær, 1994). According to the fabrication method, MZI can be roughly divided into structural types and integrated types. Structural type MZI refers to the modification of optical fiber to achieve measurable interference by exciting optical fiber inter-mode interference. A variety of structural modification methods have been proposed, such as splicing or taper stretching. In 2020, Xu et al. proposed an OFS based on LMI-MMF to realize non-wearable vital signs monitoring (Ke et al., 2021). The LMI-MMF system is composed of a 2 m long MMF and two SMFs. At the same time, all optical fibers are protected with 900 μm protective sleeves, shown in Fig. 13 (a), where a C-band ASE light source and an optical spectrum analyzer (OSA, AQ6370B) are employed (Ke et al., 2021). Compared with the commercial RR and HR sensor. The correlation between sensing value and reference value was 0.94 for RR and 0.86 for HR. Ke et al. improved the simple SMS fiber-optic HR sensor by inserting an SMF with a smaller inner diameter between the MMF and the output SMF in 2021 (Chen et al., 2021), shown in Fig. 13 (b). This SMSS structure can reduce the energy of mixed higher-order modes in the ground state during coupling, therefore enhancing the monitoring performance. At the same time, the SMSS structure reduces the requirements for optical fiber fusion, thus, the cost of SMSS fabrication is reduced. In 2021, Chen et al. proposed an SCF interferometer to non-invasively monitor HR and RR (Lyu et al., 2021). In this sensor, SMF is

Table 3
Interference-based optical fiber HR sensors.

Type		Characteristics	Sensitivity/Accuracy	Year	Ref.
MZI	Structural	• No core fiber (NCF) structure • Wavelength detection • Pulse wave measurement	Strain: 0.634 pm/με	2019	(Tan et al., 2019)
		• Dual core fiber (DCF) structure • Wavelength detection	Curvature: 18 nm/m^{-1}	2019	(Xu et al., 2020)
		• Eccentric core structure • Long-mode interference (LMI)	Pearson's Correlation:0.94 (RR)0.86 (HR)	2020	(Ke et al., 2021)
		• Single mode-multimode-small core-single mode (SMSS) structure • Toothed deformer • Snake routing diagram	Maximum error: 1 rpm (RR) 3 bpm (HR)	2021	(Chen et al., 2021)
		• Seven-core fiber (SCF) structure • Tapering down structure • No-coherence light source	Standard deviation (SD): 2.16 rpm (RR) 1.17 bpm (HR)	2021	(Lyu et al., 2021)
	Integrated	• 3×3 demodulation • Phase modulation mechanism • Package sensitization	Maximum error: 1 rpm (RR) 2 bpm (HR)	2020	(Nedoma et al., 2018)
		• 3×3 demodulation • Combined ECG to detect pre-ejection period	inter-beat interval (IBI) correlation: 0.9862	2021	(Xu et al., 2022)
		• Thin piezoelectric sheet (TPS) and phase generated carrier (PGC) demodulation • Real-time monitoring	~3.5 bpm (HR) ~1rpm (RR)	2022	(Ke et al., 2021)
Sagnac		• Dispersion-shifted fiber (DSF) • Toothed deformer • Snake routing diagram	-	2021	(Samartkit et al., 2021)
FPI		• Pulse wave detection • HR and pulse pressure (PP) measurement	1.916 mmHg/fringe (PP) Average relative error1.24% (HR)	2021	(Li et al., 2021)
		• EtCNA adhesive • PLA bracket	Strain: 2.57 pm/μN	2021	(Tan et al., 2020)

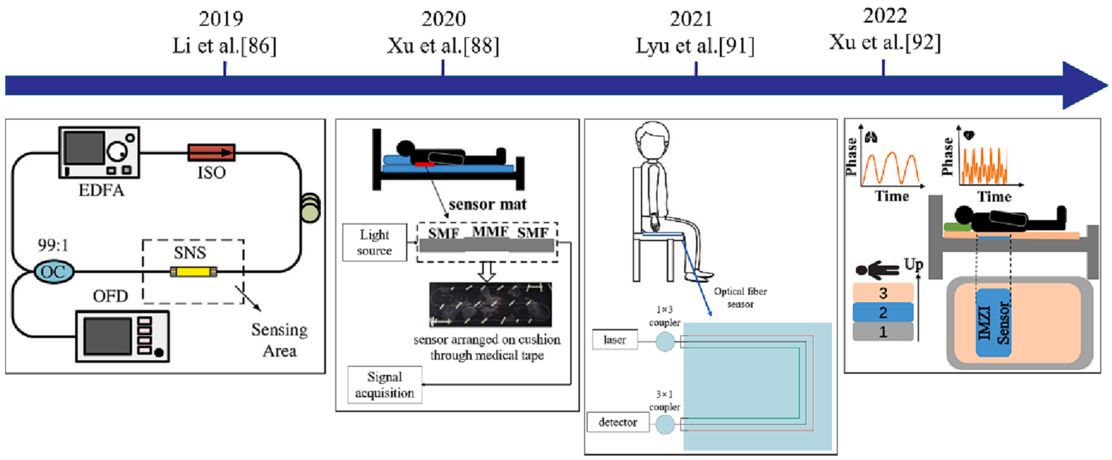

Fig. 12. Some interference-based HR OFS reported in recent years.

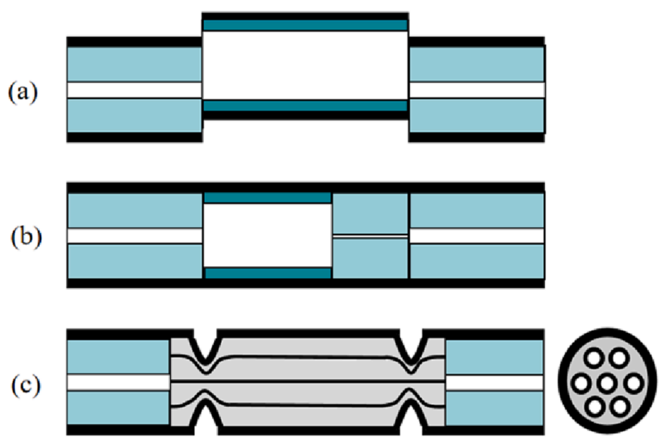

Fig. 13. Difference structural MZI HR sensor: (a) LMI-MMF (Ke et al., 2021); (b) SMSS (Chen et al., 2021), and (c) SCF (Lyu et al., 2021).

spliced at both ends of SCF, and the two ends of SCF are tapered to form dual biconical structures, shown in Fig. 13 (c). The fabricated optical fiber is arranged in a serpentine shape and sandwiched into a toothed deformer. The average error between the reference value and the measured value was 1.19 bpm for HR and 1.50 rpm for RR. In general, the structural type of MZI-based HR sensor has the characteristic of compact size, strong robustness, and relatively simple demodulation device (Chen et al., 2021), which make the sensor potentially competitive in-home medical care monitoring and other medical fields.

The integrated MZI refers to the sensor that improves the sensing sensitivity by arranging optical fibers to produce a measurable interference effect. The integrated type MZI is characterized by its good sensing performance, but the complicated demodulation device (Nedoma et al., 2018; Xu et al., 2022; Ke et al., 2021) and temperature interference (Xu et al., 2020) are factors to be considered. At present, for the integrated type, MZI is generally integrated into the mattress or cushion for monitoring. In 2020, Wang et al. designed an intelligent mattress based on optical fiber MZI for non-invasive and continuous HR monitoring (Nedoma et al., 2018). Due to the package sensitization and phase modulation mechanism applied in this mattress system, the sensor has a high sensitivity to micro-pressure. In the clinical experiment, the mattress can distinguish different exercise states (going to bed, on the bed, physical exercise on the bed, and getting out of bed), and the maximum errors are 2 bpm for HR and 1 rpm for RR. Similar to Wang, Lyu et al. used a 3×3 demodulation scheme of OFS smart cushion to measure inter-beat interval (IBI) in 2021, shown in Fig. 14 (Xu et al., 2022). Moreover, combined with ECG, this sensor can be used to evaluate the pre-ejection period (PEP), which is a measurement method to replace the expensive impedance cardiogram device. In 2022, Xu et al. proposed a fiber-optic integrated MZI (IMZI) embedded mattress assisted with TPS and PGC demodulation (Ke et al., 2021). The packaging materials, TPS, and PCG demodulation improve the sensor sensitivity. In conclusion, these integrated MZI HR monitoring systems have the advantages of being cost-effective, soft texture, dynamic monitoring capability, unobtrusive, and convenient, which has great potential in reliable homecare and hospital health monitoring.

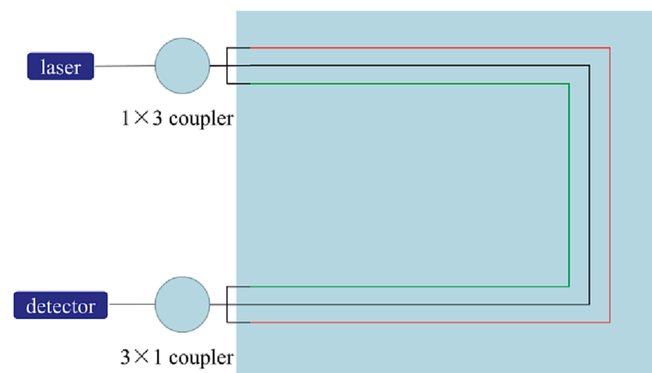

Fig. 14. MZI HR Sensor based on 120° phase difference (Xu et al., 2022).

3.2.2. OFS with Sagnac for HR monitoring

Typical Sagnac sensor is characterized by strong immunity to interference, high flexibility, and low requirement of light source coherence (Lv et al., 2021; di Virgilio, 2020). Its sensitivity is dependent on external interference frequency and loop length. Therefore; the sensing performance can be adjusted according to the requirements of practical application. The loop structure reduces the system noise caused by optical path difference, but necessitates a narrowband light source to avoid overlapping interference. Sagnac sensors are mainly used in gyroscopes (Moseley et al., 2019; Wang et al., 2010; Wang et al., 2021). In recent years; other applications in the sensing part have also made progress; such as HR monitoring. In 2021, Ke et al. proposed an intelligent mattress based on an unbalanced optical fiber Sagnac loop sensor structure to detect vital signs such as RR and HR in real time, shown in Fig. 15 (Samartkit et al., 2021). The sensitivity and stability of the system are enhanced by the unbalanced Sagnac loop structure formed by two different types of optical fibers and the micro-bend and serpentine arrangement of optical fibers in the mattress. The measured data of this

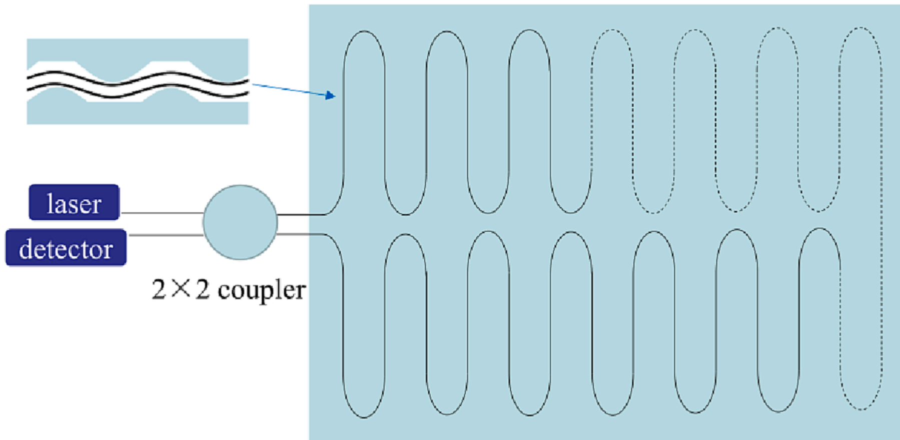

Fig. 15. Optical fiber HR sensor based on tooth deformer and unbalanced Sagnac loop structure (Samartkit et al., 2021).

mattress is highly correlated with the reference data. Therefore; it has broad application prospects in the medical and health field.

3.2.3. OFS with FPI for HR monitoring

FPI is characterized by flexibility and compact device. As an interferometer with optical path structure, FPI will be more independent of environmental disturbances than those with a non-common optical path structure and yield clearer results when environmental disturbances are present (Wu et al., 1992). Compared with other dual optical fiber pairings, the configuration requirement of FPI is not high due to the single optical fiber structure. In 2021, Samartkit et al. fabricated an optical fiber FPI for non-invasive measurement of HR and pulse pressure (PP) (Li et al., 2021), shown in Fig. 16 (a). The FPI is simple in design and demodulates the output by counting interference fringes. The experimental results show that the sensitivity of FPI measured by PP is ~1.916 mmHg/stripe. For HR monitoring, the average difference was 1.24 % compared with the reference value. Li et al. proposed an in-fiber FPI sensor for HR monitoring in 2021 (Tan et al., 2020), shown in Fig. 16 (b). The FPI sensor was fixed in the capillary by ethyl alpha-cyanoacrylate (EtCNA) adhesive and the OFS is installed on a specially

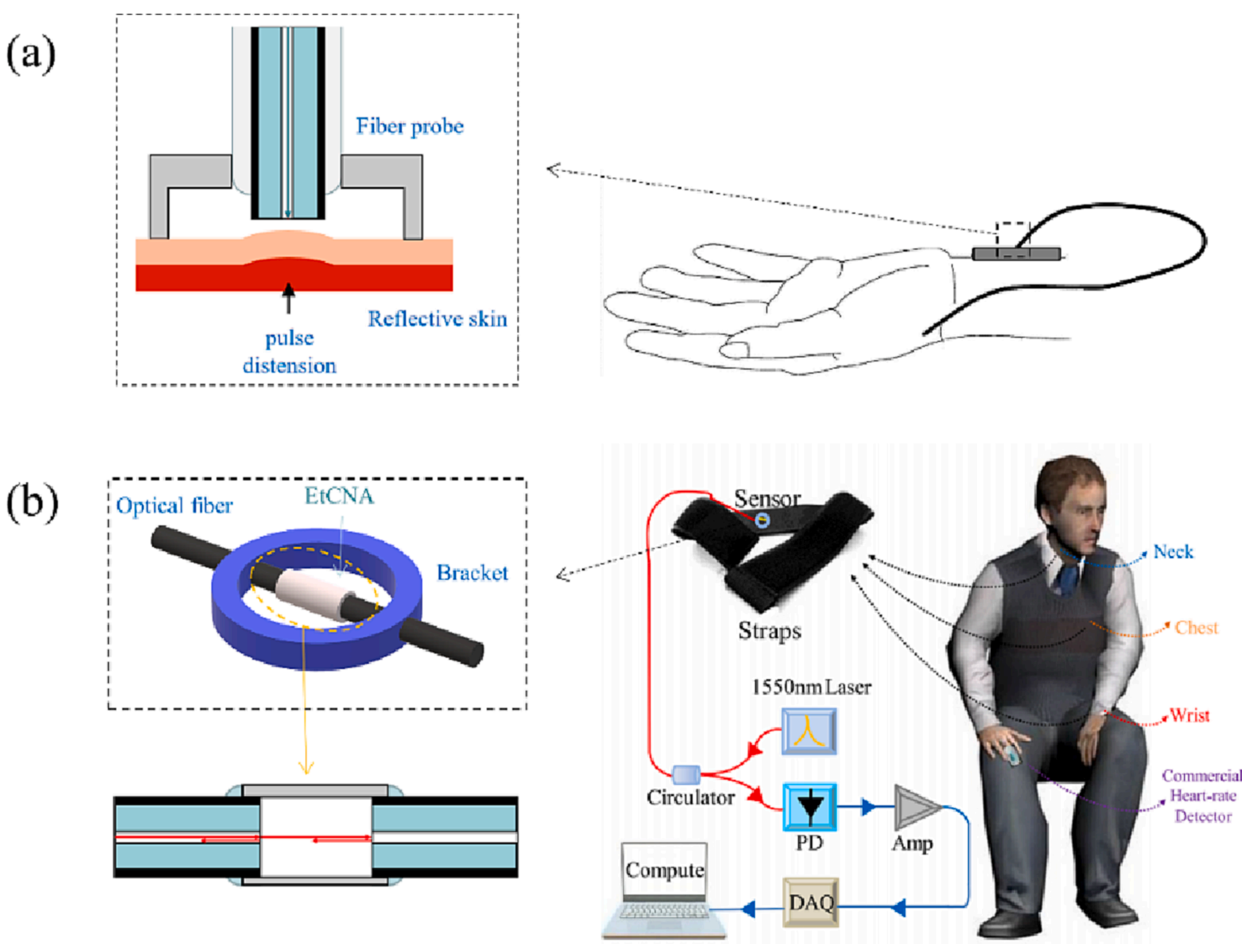

Fig. 16. FPI HR sensor: (a)PW-based (Li et al., 2021) and (b) ACG based (Tan et al., 2020).

designed bracket to obtain stable data. Based on the low Young's modulus of EtCNA material and the bracket, the sensor can be placed in different parts of the human body, such as the wrist and chest, and detect low-frequency vibration with high sensitivity. Due to its small size and high sensitivity, FPI is expected to be widely used in HR monitoring.

3.3. OFS with specklegram for HR monitoring

For FSS in HR monitoring, the measurement method is similar to intensity-based, that is, based on the correlation between the change of light intensity and the body movement caused by heartbeat. The difference is that the (local) light intensity change of FSS is caused by the change of interference mode, and the correlation algorithm is applied for analysis. In FSSs, the structures and characteristics of fiber specklegram are determined by the light source and transmission MMF. Therefore, different specifications of MMF can be used for different requirements of measurement, allowing for flexible sensing. In addition, FSS has multiplexing capability because it can transmit modes with angle or wavelength division multiplexing. Specifically, for FSS, with a large number of existing modes, the light field reconstructed from the speckle pattern will be weak enough that the change of fiber status in different aspects can be regarded as orthogonal status (Podbreznik et al., 2013). Thus, through the orthogonal status, by using different reference beam angles or wavelengths or both, we can multiplex the fiber specklegram. An FSS only needs a camera to record the information of speckle, thus creating a possible compact and low-cost interrogation system. In addition, with the continuous development of CCD camera technology, the frames per second (fps) of such devices increase significantly, which makes the high acquisition frequency of FSS. At the same time, the use of CCD as an interrogator also makes the cost of the sensing system greatly reduced. To sum up, FSS has potential application value in HR sensing. Table 4 and Fig. 17 describe the latest FSS HR sensors.

In 2013, Podbreznik et al. proposed a kind of POF based FSS for HR and RR monitoring (Mokhtar et al., 2012); shown in Fig. 18. Due to the low-cost components of the sensing system, such as commercial 650 nm laser diode, POF and linear optical sensor array, the FSS is cost-efficient. Compare the data obtained from FSS with ECG signals and evaluate the effectiveness. The results show that the sensor has high precision and sensitivity, and mean delay between FSS and ECG signal is less than 1.3 s. In 2015, Benevides et al. proposed a portable and unobtrusive HR FSS (Rodríguez-Cuevas et al., 2017). The FSS monitors the HR by measuring the wrist pulse and collecting images using a single board computer. Therefore; the equipment is compact. Welch power spectrum estimate and threshold analysis are used to extract HR signals and the results show that the average error is 1.31 bpm when welch is used. Rodríguez-Cuevas et al. analyzed the effect of HR FSS when placed at different positions and using different data processing methods in 2017 (Efendioglu, 2017). At the same time; the long-term monitoring capability of FSS in the optimal position is tested. The results shown that the relative HR instantaneous error is below 3 % and the mean error is below 10 %. In 2020, Zhan et al. proposed a HR measurement system based on FSS (Tavares et al., 2022). The identification of different frequency vibration by FSS is verified. Then; different types of fibers with different diameters are used for sensing, and the relationship between them and sensing sensitivity is studied. Finally, a 200 μm POF and a 500 μm silica MMF were selected to measure HR, with obvious regular pulse peak appeared. In general, FSS has potential application value in HR detection with advantageous features such as cost-efficient, easy connectivity, high flexibility, and better performance.

3.4. OFS with FBG for HR monitoring

In HR measurement, FBG is mainly used for BCG. Since the FBG wavelength shift is greatly affected by temperature and strain, some processing is required to overcome the cross-sensitivity effect (Nedoma et al., 2017). At present, the main solution is to package FBG. Generally, polymer materials are used as the packaging materials of FBG. On the one hand, the high flexibility and toughness of polymer can make FBG close to the surface of the human body and increase the sensing performance. On the other hand, polymer packaging can protect the relatively fragile FBG sensing part and increase the measurable range. However, FBG requires high fabrication requirements, and its interrogator also needs more sophisticated instruments such as spectrometer, which is also more expensive. Therefore, the cost of the sensing system should be considered in actual use. Table 5 and Fig. 19 describes the recent FBG HR sensors.

The high sensitivity of FBG and the diversity of packaging materials make the fabrication of HR sensors based on FBG very flexible. In 2017, Nedoma et al. proposed a non-invasive OFS for vital signs monitoring, which can measure HR and skin temperature at the same time (Nedoma et al., 2019). As shown in Fig. 20 (a), because different positions in the trapezoidal plane structure of the polymer, the two FBGs encapsulated in the PDMS material have different responses to temperature and stress. Therefore, the inherent strain-temperature cross-sensitivity of OFS can be demodulated by detecting the two different wavelength shifts, thus achieving the effect of multi-parameter monitoring. The interrogator system is mainly implemented by an OSA with sampling frequency of 250 Hz and through Bland-Altman analysis, which shows the consistency between the two measurement methods, 95.34 % of the differences between the proposed sensor and reference sensor were within ± 1.96 SD measured by HR, and 95.01 % of the differences were within ± 1.96 SD measured by RR. The max error of body surface temperature is less than 0.2℃ and the relative error in Celsius is less than 0.55 %. Utilizing the EMI characteristic of optical fiber, in 2019, Nedoma et al. proposed a solution to continuously monitor HR and RR in a magnetic resonance imaging (MRI) environment through an FBG sensor (Lo Presti et al., 2019). The FBG was encapsulated in fiberglass, shown in Fig. 20 (b). Its package and structure make the sensor have a very compact size (30 × 10 × 0.8 mm) and low weight (2 g). The interrogator unit used is FBGuard, a kind of spectral conventional instrument with wavelength range 1510–1590 nm, wavelength resolution ≤ 1 pm and output power 1 mW. and the relative error of the sensor is less than 5 % (4.64 % for RR

Table 4
Specklegram-based optical fiber HR sensors

Characteristic	Image processing	Data processing	Sensitivity	Year	Ref.
Cost-efficient	Phase shifting of consecutive images	• Morlet wavelet extract signal (HR) • Band-pass filtering (RR)	Sensitivities of 99.4%± 0.6% (HR) 95.3%± 3% (RR)	2013	(Mokhtar et al., 2012)
Portable and unobtrusive	Differential processing method	• Welch power spectral density estimate • Threshold analysis.	Mean error:1.31 bpm *(welch) and* 6 bpm *(threshold)*	2015	(Rodríguez-Cuevas et al., 2017)
Long term monitoring	Differential processing method	• Smooth processing • First-order Fourier transform • Convolution by sinusoid	Relative error below 3% (instant) and 10% (long term)	2017	(Efendioglu, 2017)
Comparison for different fibers	NIPC	• Fast Fourier transform	-	2020	(Tavares et al., 2022)

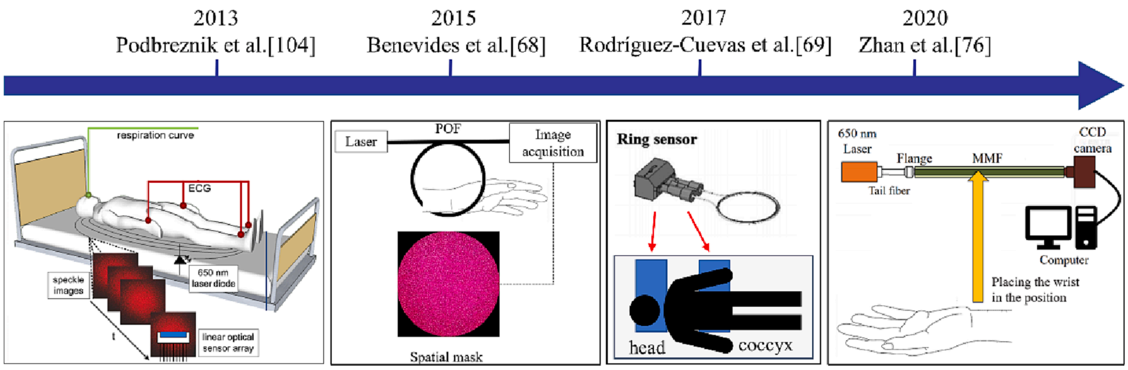

Fig. 17. Some specklegram-based HR OFS reported in recent years.

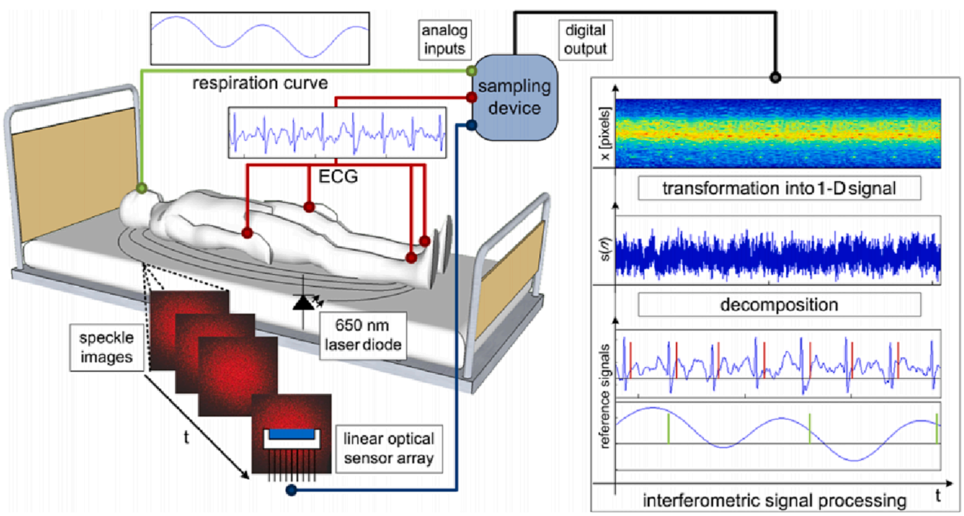

Fig. 18. The schematic diagram of cost-efficient POF based FSS (Mokhtar et al., 2012).

Table 5
FBG-based optical fiber HR sensors.

Size (length×width×thickness)	Package Material	Characteristics	Sensitivity/ Accuracy	Year	Ref.
70 mm × 40 mm × 4 mm	PDMS	• Strain and temperature cross sensitivity is solved by encapsulation • Multi parameter simultaneous measurement	Bland-Altman analysis: HR: 95.34% RR: 95.01% Maximum relative error of temperature: 0.55 %	2017	(Nedoma et al., 2019)
30 mm × 10 mm × 0.8 mm	Fiberglass	• Equipment miniaturization through encapsulation • Innovative FBG encapsulation method.	Bland-Altman analysis: HR: 95.13% RR: 95.36%	2019	(Lo Presti et al., 2019)
90 mm × 24 mm × 1 mm	Dragon Skin@20, Smooth-on	• Flexible, fit to body surface	Temperature: 0.012 nm/℃ Strain: 0.125 nm/mε	2019	(Cheng et al., 2020)
70 mm × 5 mm × 1 mm (Wrist) 20 mm × 20 mm × 1 mm (Abdomen)	silicone rubber	• First-time fabrication of FBG in all ZEONEX-based SMPOFs	Temperature: (just produced) -0.02547 nm/°C Strain: (just produced) 1.4 nm/mε	2020	(Ferraro et al., 2021)
41 mm × 15 mm × 3 mm	Dragon Skin30, Smooth-on	• Dynamic threshold (DT) and neural network (NN) algorithms • Implantation into the heart • Vivo and in-vivo test for mammal	HR error in in-vivo test:0.1 bpm (DT)0.6 bpm (NN)	2021	(Lo Presti et al., 2021)
230 mm × 36 mm × 1 mm	Dragon Skin@20, Smooth-on	• SCG signal measurement • Multiple FBGs for reduce error	Mean absolute error: 0.81 bpm	2021	(Bonefacino et al., 2018)
400 mm × 30 mm × 2 mm	elastic material	• Fused deposition modeling	Mean absolute error: 0.8 bpm	2022	(Kuang et al., 2022)

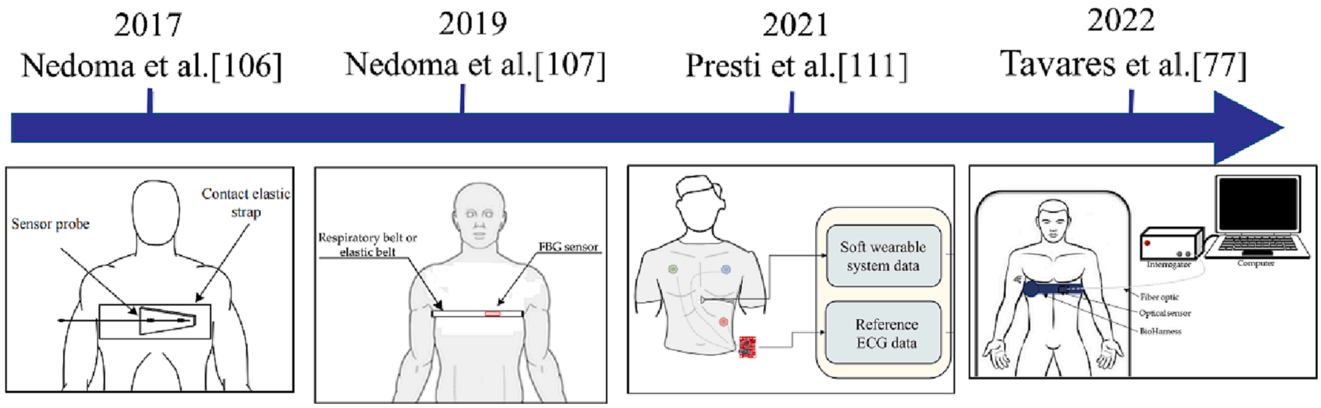

Fig. 19. Some FBG-based HR OFS reported in recent years.

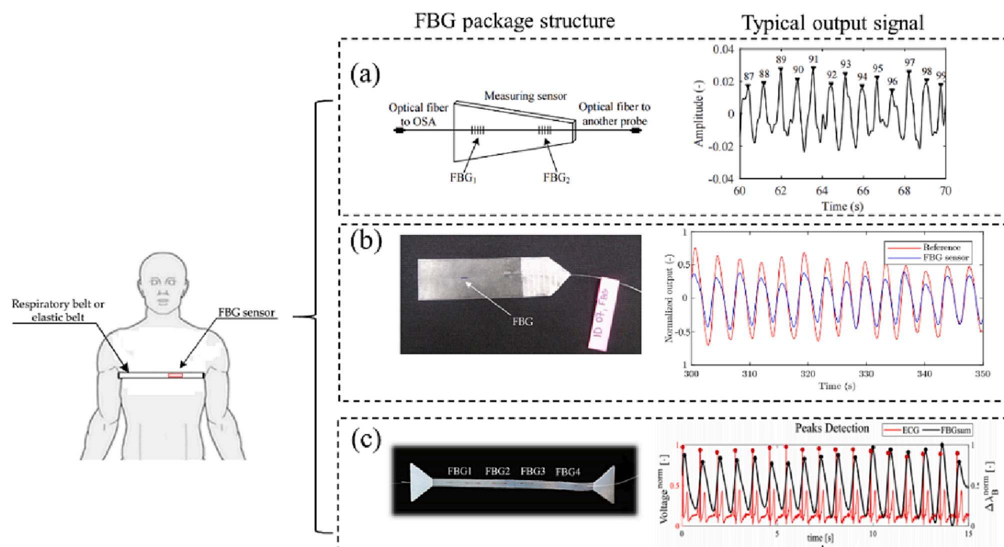

Fig. 20. FBG HR Sensor and their output signals: (a) trapezoidal FBG sensor (Nedoma et al., 2019), (b) compact sensors for MRI environments (Lo Presti et al., 2019), and (c) multi-point simultaneous measurements (Bonefacino et al., 2018).

and 4.87 % for HR). In 2021, Presti et al. proposed a soft wearable multiple FBG systems for human HR monitoring (Bonefacino et al., 2018). The FBGs which allow multi-point simultaneous measurements are linearly packaged in silicone rubber (180 mm × 8 mm × 1 mm) and the trapezoidal structure is added at both ends to fit closely against the human body (the oversize 230 mm × 36 mm × 1 mm), shown in Fig. 20 (c). The sampling rate of the interrogator (Si255, Micron Optics Inc.) is 1 kHz, the average strain sensitivity of the FBGs used is 0.045 nm/mε and compared the sum of HR data output by each FBG with the reference ECG signal, the mean absolute error of HR reaches 0.81 bpm. With the improvement of the material preparation process, new FBG materials, such as polymer optical fiber Bragg grating (POFBG), appear in FBG sensing (Bonefacino et al., 2018). In 2020, Cheng et al. fabricated an HR sensor based on a new material POFBG (Ferraro et al., 2021). A manufacturing method of SM-POF based on ZEONEX is proposed. On this basis, POFBG with better sensing performance than traditional FBG is obtained by laser writing. In this HR sensor, POFBG is embedded in silicone rubber for measurement, two sizes of packages are fabricated for placement on the wrist (70 × 5 × 1 mm) and chest (20 × 20 × 1 mm). The interrogator (Si155, Micron Optics Inc.) with a resolution of 1 pm is used, the results show that for ZEONEX-POFBG, the wavelength shift caused by heartbeat can reach 4 pm, which is 4 times that of the reference silica FBG sensor. There are also studies on the direct implantation of FBG into the heart for HR measurement. In 2021, Ferraro et al. proposed an implantable flexible FBG sensor for sensing the mechanical motion of the heart (Lo Presti et al., 2021). The FBG sensing part is composed of two elastic elements divided by three rigid aluminum flats. The function of the aluminum flat is to insert the sensing part into the epicardial surface of the left ventricle (LV). The interrogator used is FBG-Scan 904 (FBGS, Geel, BE) with a 10 pm resolution. Two algorithms (dynamic threshold (DT) and neural network (NN)) are proposed to extract HR data, and the ability to track heart activity in real time was tested through vivo and in vivo studies in large mammals. The minimum error of tracking HR was 2.7 ± 0.7 bpm and the errors of the two algorithms were 0.1 bpm and 0.6 bpm for DT and NN, respectively. In general, the FBG HR sensor is developing in the direction of small size, high robustness, and easy fabrication based on high accuracy. At the same time, it is also one of the concerns to reduce the cost of FBG writing and demodulation/interrogator.

4. Conclusion

OFS has attracted wide attention because of its flexibility, chemical inertness, and anti-electromagnetic interference. With these advantages, OFS has made progress in the field of HR monitoring. However, the research on OFS HR sensing is still in the experimental stage. The difficulty lies in commercializing this OFS research, which requires improvement in many aspects, such as sensing performance, demodulation mode, and user experience. In terms of sensing performance, as the HR signal is weak (compared with the RR signal), signal amplification is required to improve sensitivity. At the same time, the stability of long-term monitoring and robustness to the environment also need to be considered. For the signal demodulation mode, the traditional high-cost demodulation device can be replaced by an auxiliary algorithm. This has been widely used and commercialized in cameras, so this is a feasible direction. The algorithm can also demodulate multiple parameters without additional hardware cost. Another method is to use multiple sensors, but this will increase the complexity of the device, which *may be* not conducive to equipment miniaturization and cost. As for user experience, security and portability should be considered. The intrinsic safety of optical fiber is an important advantage of OFS. The miniaturization of the sensing part has been studied. However, desktop instruments (such as light sources, spectrometers, photoelectric detectors, etc.) limit the feasibility of portable HR monitoring. Smaller demodulation systems and packages, such as the optical fiber wearable sensor design based on mobile phones, facilitate the use of OFS for portable HR monitoring.

This paper introduces several main technologies of optical fiber HR sensors, such as intensity-based, interference-based, specklegram-based and FBG-based. Intensity-based OFS is most widely used due to the advantages of low cost and ease of fabrication. However, additional processing is usually required to enhance sensitivity or signal-to-noise ratio. Interference-based HR sensor is characterized by high sensitivity and flexibility though requirements for interference devices and demodulation devices are the factors limiting their applications. Specklegram-based HR sensor has a bright application prospect in the future because of its low demodulation and light source requirements, which lead to the low cost and high compactness of sensing system. FBG-based HR sensor is developing in the direction of small size and easy fabrication based on high accuracy, however, the high cost of interrogator limits its applications. The application of OFS in HR monitoring in recent years is introduced and discussed. Compared with the current mature commercial HR monitoring devices, especially the miniaturized and portable ECG commercial instruments that have emerged in recent years, and the monitoring function based on optical plethysmography in smartwatches, the OFS for HR monitoring still needs to be further developed. In conclusion, different types of OFS have their own advantages and shortcomings when it comes to HR detection, and the research potential of OFS enables it to be discussed and optimized in the future.

CRediT authorship contribution statement

Runjie He: Writing – original draft. **Lingyu Shen:** Writing – original draft. **Zhuo Wang:** Writing – original draft. **Guoqing Wang:** Writing – review & editing. **Hang Qu:** Writing – review & editing. **Xuehao Hu:** Writing – review & editing. **Rui Min:** Writing – review & editing, Project administration, Funding acquisition.

Declaration of Competing Interest

The authors declare that they have no known competing financial interests or personal relationships that could have appeared to influence the work reported in this paper.

Data availability

No data was used for the research described in the article.

Acknowledgement

Guangdong Basic and Applied Basic Research Foundation (2021A1515011997); National Natural Science Foundation of China (62003046, 62111530238); The Fonds de la Recherche Scientifique (F.R.S.-FNRS) under the Postdoctoral Researcher grant (Chargé de Recherches) of Xuehao Hu; Special Funds for the Cultivation of Guangdong College Students' Scientific and Technological Innovation ("Climbing Program" Special Funds) (pdjh2022a0684);Special project in key field of Guangdong Provincial Department of Education (2021ZDZX1050); The Innovation Team Project of Guangdong Provincial Department of Education (2021KCXTD014).

References

Alametsä, J., Värri, A., Viik, J., Hyttinen, J., Palomäki, A., 2009. Ballistocardiogaphic studies with acceleration and electromechanical film sensors. Med. Eng. Phys. 31 (9), 1154–1165. https://doi.org/10.1016/J.MEDENGPHY.2009.07.020.

Al-Handarish, Y., Omisore, O.M., Igbe, T., Han, S., Li, H., Du, W., Zhang, J., Wang, L., 2020. A survey of tactile-sensing systems and their applications in biomedical engineering. Adv. Mater. Sci. Eng. 2020, 1–17.

Amanzadeh, M., Aminossadati, S.M., Kizil, M.S., Rakić, A.D., 2018. Recent developments in fibre optic shape sensing. Measurement 128, 119–137. https://doi.org/10.1016/J.MEASUREMENT.2018.06.034.

Arifin, A., Lebang, A.K., Yunus, M., Dewang, S., Idris, I., Tahir, D., 2019. Measurement heart rate based on plastic optical fiber sensor. J. Phys. Conf. Ser. 1170 (1) https://doi.org/10.1088/1742-6596/1170/1/012074.

Asif, I.M., Drezner, J.A., 2016. Cardiovascular screening in young athletes: evidence for the electrocardiogram. Curr. Sports Med. Rep. 15 (2), 76–80. https://doi.org/10.1249/JSR.0000000000000247.

N. R. Avula, T. Dighe, A. Sajgure, C. Bale, and P. Wakhare, "Evaluation of role of heart rate variability with holter monitoring in chronic kidney disease," Int. J. Res. Med. Sci., vol. 8, no. 6, p. undefined-undefined, May 2020, doi: 10.18203/2320-6012.IJRMS20202264.

A. B. Benevides, A. Frizera, A. Cotrina, M. R. N. Ribeiro, M. E. v. Segatto, and M. J. Pontes, "Unobtrusive heart rate monitor based on a fiber specklegram sensor and a single-board computer," 24th International Conference on Optical Fibre Sensors, vol. 9634, p. 963468, 2015, doi: 10.1117/12.2194618.

Bonefacino, J., Tam, H., Glen, T., Cheng, X., Pun, C., Wang, J., Lee, P., Tse, M., Boles, S., 2018. Ultra-fast polymer optical fibre Bragg grating inscription for medical devices. Light Sci. Appl. 7 (3), 17161. https://doi.org/10.1038/LSA.2017.161.

Boutouyrie, P., Bussy, C., Lacolley, P., Girerd, X., Laloux, B., Laurent, S., 1999. Association between local pulse pressure, mean blood pressure, and large-artery remodeling. Circulation 100 (13), 1387–1393. https://doi.org/10.1161/01.CIR.100.13.1387.

Broadway, C., Min, R., Leal-Junior, A.G., Marques, C., Caucheteur, C., 2019. Toward commercial polymer fiber bragg grating sensors: review and applications. J. Lightwave Technol. 37 (11), 2605–2615. https://doi.org/10.1109/JLT.2018.2885957.

Cardona-Morrell, M., Prgomet, M., Turner, R.M., Nicholson, M., Hillman, K., 2016. Effectiveness of continuous or intermittent vital signs monitoring in preventing adverse events on general wards: a systematic review and meta-analysis. Int. J. Clin. Pract. 70 (10), 806–824. https://doi.org/10.1111/IJCP.12846.

Chen, Z., Lau, D., Teo, J.T., Ng, S.H., Yang, X., Kei, P.L., 2014. Simultaneous measurement of breathing rate and heart rate using a microbend multimode fiber optic sensor. J. Biomed. Opt. 19 (5), 057001 https://doi.org/10.1117/1.JBO.19.5.057001.

Chen, G., Yuan, X., Zhang, Y., Song, X., 2021. A new approach to HR monitoring using photoplethysmographic signals during intensive physical exercise. Phys. Eng. Sci. Med. 44 (2), 535–543. https://doi.org/10.1007/S13246-021-01003-4.

Chen, W., Zhang, Y., Yang, H., Qiu, Y., Li, H., Chen, Z., Yu, C., 2021. Non-invasive measurement of vital signs based on seven-core fiber interferometer. IEEE Sens. J. 21 (9), 10703–10710. https://doi.org/10.1109/JSEN.2021.3061443.

Cheng, X., Gunawardena, D.S., Pun, C.-F.-J., Bonefacino, J., Tam, H.-Y., 2020. Single nanosecond-pulse production of polymeric fiber Bragg gratings for biomedical applications. Opt. Express 28 (22), 33573. https://doi.org/10.1364/OE.408744.

Choi, S.J., Kim, Y.C., Song, M., Pan, J.K., 2014. A self-referencing intensity-based fiber optic sensor with multipoint sensing characteristics. Sensors (Switzerland) 14 (7), 12803–12815. https://doi.org/10.3390/S140712803.

Chowdhury, S.S., Hyder, R., Hafiz, M.S.B., Haque, M.A., 2018. Real-time robust heart rate estimation from wrist-type PPG signals using multiple reference adaptive noise cancellation. IEEE J. Biomed. Health Inform. 22 (2), 450–459.

Corodeanu, S., Chiriac, H., Radulescu, L., Lupu, N., 2014. Magneto-impedance sensor for quasi-noncontact monitoring of breathing, pulse rate and activity status. J. Appl. Phys. 115 (17), 17A301.

C. B. Cross, J. A. Skipper, and D. Petkie, "Thermal imaging to detect physiological indicators of stress in humans," Proc. SPIE 8705, Thermosense: Thermal Infrared Applications XXXV, p. 87050I, May 2013, doi: 10.1117/12.2018107.

Dabaghyan, M., Zhang, S.H., Ward, J., Kwong, R.Y., Stevenson, W.G., Watkins, R.D., Tse, Z.T., Schmidt, E.J., 2016. 3T cardiac imaging with on-line 12-lead ECG monitoring. J. Cardiovasc. Magn. Reson. 18 (S1) https://doi.org/10.1186/1532-429x-18-s1-p212.

di Virgilio, A.D.V., 2020. Sagnac Gyroscopes and the GINGER Project. Front. Astron. Space Sci. 7 https://doi.org/10.3389/FSPAS.2020.00049.

Efendioglu, H.S., 2017. A review of fiber-optic modal modulated sensors: specklegram and modal power distribution sensing. IEEE Sens. J. 17 (7), 2055–2064. https://doi.org/10.1109/JSEN.2017.2658683.

Fajkus, M., Nedoma, J., Martinek, R., Brablik, J., Vanus, J., Novak, M., Zabka, S., Vasinek, V., Hanzlikova, P., Vojtisek, L., 2019. MR fully compatible and safe FBG breathing sensor: a practical solution for respiratory triggering. IEEE Access 7, 123013–123025.

Faust, O., Lei, N., Chew, E., Ciaccio, E.J., Acharya, U.R., 2020. A smart service platform for cost efficient cardiac health monitoring. Int. J. Environ. Res. Public Health 17 (17), 1–18. https://doi.org/10.3390/IJERPH17176313.

Ferraro, D., D'Alesio, G., Camboni, D., Zinno, C., Costi, L., Haberbusch, M., Aigner, P., Maw, M., Schloglhofer, T., Unger, E., Aliperta, A., Bernini, F., Casieri, V., Terlizzi, D., Giudetti, G., Carpaneto, J., Pedrizzetti, G., Micera, S., Lionetti, V., Moscato, F., Massari, L., Oddo, C.M., 2021. Implantable fiber Bragg grating sensor for continuous heart activity monitoring: ex-vivo and in-vivo validation. IEEE Sens. J. 21 (13), 14051–14059.

Friebele, E.J., Askins, C.G., Miller, G.A., Peele, J.R., Wasserman, L.R., 2004. Optical fiber sensors for spacecraft: applications and challenges. Photonics for Space Environments IX 5554, 120. https://doi.org/10.1117/12.562393.

Ge, J., Cheng, X., Zhao, C., Gui, K., Zhang, W., Cheikh, F., Ye, L., 2020. Reflected light intensity-modulated continuous liquid level sensor based on oblique end face coupling optical fibers. IEEE Sens. J. 20 (8), 4229–4236. https://doi.org/10.1109/JSEN.2019.2962610.

Ghosh, S.K., Ponnalagu, R.N., Tripathy, R.K., Acharya, U.R., Tang, C., 2020. Deep Layer kernel sparse representation network for the detection of heart valve ailments from the time-frequency representation of PCG recordings. Biomed Res. Int. 2020, 1–16.

Gordon, J.W., 1877. Certain molar movements of the human body produced by the circulation of the blood. Available J. Anat. Physiol. 11 (Pt 3), 533–536. https://www.mendeley.com/catalogue/5b6e8df0-1c33-3b1b-8880-2a0e3244f805/.

Guzmán-Sepúlveda, J.R., Guzmán-Cabrera, R., Castillo-Guzmán, A.A., 2021. Optical sensing using fiber-optic multimode interference devices: a review of nonconventional sensing schemes. Sensors 21 (5), 1–21. https://doi.org/10.3390/S21051862.

P. Han et al., "Low-cost plastic optical fiber sensor embedded in mattress for sleep performance monitoring," Opt. Fiber Technol., vol. 64, 2021, doi: 10.1016/J.YOFTE.2021.102541.

Hao, J., Jayachandran, M., Kng, P.L., Foo, S.F., Aung Aung, P.W., Cai, Z., 2010. FBG-based smart bed system for healthcare applications. Front. Optoelectron. 3 (1), 78–83. https://doi.org/10.1007/S12200-009-0066-0.

Hayashi, K., Koshiba, M., Tsuji, Y., Yoneta, S., Kaji, R., 1998. Combination of beam propagation method and mode expansion propagation method for bidirectional optical beam propagation analysis. J. Lightwave Technol. 16 (11), 2040–2045. https://doi.org/10.1109/50.730368.

He, R., Teng, C., Kumar, S., Marques, C., Min, R., 2022. Polymer optical fiber liquid level sensor: a review. IEEE Sens. J. 22 (2), 1081–1091. https://doi.org/10.1109/JSEN.2021.3132098.

Hu, X., Kinet, D., Chah, K., Pun, C.-F.-J., Tam, H.-Y., Caucheteur, C., 2017. Bragg grating inscription in PMMA optical fibers using 400-nm femtosecond pulses. Opt. Lett. 42 (14), pp. https://doi.org/10.1364/ol.42.002794.

Huang, W., Ying, T., Chin, W., Baskaran, L., Marcus, O., Yeo, K., Kiong, N., 2022. Application of ensemble machine learning algorithms on lifestyle factors and wearables for cardiovascular risk prediction. Sci. Rep. 12 (1) https://doi.org/10.1038/S41598-021-04649-Y.

J. Jiang, N. Zhang, R. Min, X. Cheng, H. Qu, X. Hu, "Recent achievements on grating fabrications in polymer optical fibers with photosensitive dopants: a review," Polymers (Basel), vol. 14, no. 2, p. undefined-undefined, 2022, doi: 10.3390/POLYM14020273.

Jiang, P., Zhao, S., Zhu, R., 2015. Smart sensing strip using monolithically integrated flexible flow sensor for noninvasively monitoring respiratory flow. Sensors (Switzerland) 15 (12), 31738–31750. https://doi.org/10.3390/S151229881.

Kause, J., Smith, G., Prytherch, D., Parr, M., Flabouris, A., Hillman, K., 2004. A comparison of antecedents to cardiac arrests, deaths and emergency intensive care admissions in Australia and New Zealand, and the United Kingdom – The ACADEMIA study. Resuscitation 62 (3), 275–282. https://doi.org/10.1016/J.RESUSCITATION.2004.05.016.

Ke, C., Cai, Y., Zhao, T., Li, Z., 2021. Research on smart mattress based on fiber unbalanced Sagnac loop. IOP Conf. Ser. Earth Environ. Sci. 769 (4), 042039.

Ke, C., Cai, Y., Zhao, T., Li, Z., 2021. Research on intelligent mattress based on improved SMS structure sensing fiber. 7th IOP Conf. Ser. Earth Environ. Sci. 1802 (2), 022023.

Khan, Y., Ostfeld, A.E., Lochner, C.M., Pierre, A., Arias, A.C., 2016. Monitoring of vital signs with flexible and wearable medical devices. Adv. Mater. 28 (22), 4373–4395. https://doi.org/10.1002/ADMA.201504366.

Khosrow-Khavar, F., Tavakolian, K., Blaber, A.P., Zanetti, J.M., Fazel-Rezai, R., Menon, C., 2015. Automatic annotation of seismocardiogram with high-frequency precordial accelerations. IEEE J. Biomed. Health Inform. 19 (4), 1428–1434. https://doi.org/10.1109/JBHI.2014.2360156.

Knudsen, S., Bløtekjær, K., 1994. An ultrasonic fiber-optic hydrophone incorporating a push-pull transducer in a sagnac interferometer. J. Lightwave Technol. 12 (9), pp. https://doi.org/10.1109/50.320954.

Koyama, Y., Nishiyama, M., Watanabe, K., 2018. Smart textile using hetero-core optical fiber for heartbeat and respiration monitoring. IEEE Sens. J. 18 (15), 6175–6180. https://doi.org/10.1109/JSEN.2018.2847333.

Kuang, R., Ye, Y., Chen, Z., He, R., Savović, I., Djordjevich, A., Savović, S., Ortega, B., Marques, C., Li, X., Min, R., 2022. Low-cost plastic optical fiber integrated with smartphone for human physiological monitoring. Opt. Fiber Technol. 71, 102947.

Leal-Junior, A.G., Díaz, C.R., Leitão, C., Pontes, M.J., Marques, C., Frizera, A., 2019. Polymer optical fiber-based sensor for simultaneous measurement of breath and heart rate under dynamic movements. Opt. Laser Technol. 109, 429–436. https://doi.org/10.1016/J.OPTLASTEC.2018.08.036.

Leal-Junior, A.G., Frizera, A., Marques, C., Pontes, M.J., 2020. Optical fiber Specklegram sensors for mechanical measurements: a review. IEEE Sens. J. 20 (2), 569–576. https://doi.org/10.1109/JSEN.2019.2944906.

Lee, H.S., Cho, K.W., Kim, H.Y., Ahn, Y.M., 2020. Chamber-specific regulation of atrial natriuretic peptide secretion in cardiac hypertrophy: atrial wall dynamics in the ANP secretion. Pflug. Arch. Eur. J. Phy. 472 (6), pp. https://doi.org/10.1007/s00424-020-02377-2.

S. Leonhardt, D. Teichmann, "Fusing non-contact vital sign sensing modalities - first results," 40th Annual International Conf Proc IEEE Eng Med Biol Soc, pp. 5378–5381, 2018, doi: 10.1109/EMBC.2018.8513639.

Li, Y., Dong, B.o., Chen, E., Wang, X., Zhao, Y., 2021. Heart-rate monitoring with an ethyl alpha-cyanoacrylate based fiber fabry-perot sensor. IEEE J. Sel. Top. Quantum Electron. 27 (4), 1–6.

Li, T., Wu, D., Khyam, M.O., Guo, J., Tan, Y., Zhou, Z., 2022. Recent advances and tendencies regarding fiber optic sensors for deformation measurement: a review. IEEE Sens. J. 22 (4), 2962–2973. https://doi.org/10.1109/JSEN.2021.3138091.

Li, K., Xia, L., Yi, H., Li, S., Wu, Y., Song, Y., 2019. Optical active fiber sensing technique based on the lasing wavelength demodulation for monitoring the human respiration and pulse. Sens Actuators A Phys 296, 45–51. https://doi.org/10.1016/J.SNA.2019.06.045.

Lin, J., Fu, R., Zhong, X., Yu, P., Tan, G., Li, W., Zhang, H., Li, Y., Zhou, L., Ning, C., 2021. Wearable sensors and devices for real-time cardiovascular disease monitoring. Cell Rep. Phys. Sci. 2 (8), 100541.

Lo Presti, D., Massaroni, C., D'Abbraccio, J., Massari, L., Caponero, M., Longo, U.G., Formica, D., Oddo, C.M., Schena, E., 2019. Wearable system based on flexible FBG for respiratory and cardiac monitoring. IEEE Sens. J. 19 (17), 7391–7398.

Lo Presti, D., Santucci, F., Massaroni, C., Formica, D., Setola, R., Schena, E., 2021. A multi-point heart rate monitoring using a soft wearable system based on fiber optic technology. Sci. Rep. 11 (1) https://doi.org/10.1038/S41598-021-00574-2.

Lv, J., Fang, N., Wang, C., Wang, L., 2021. Location method of Sagnac distributed optical fiber sensing system based on CNNs ensemble learning. Opt. Laser Technol. 138, 106841 https://doi.org/10.1016/J.OPTLASTEC.2020.106841.

W. Lyu, S. Chen, F. Tan, and C. Yu, "Vital Signs Monitoring Based on Interferometric Fiber Optic Sensors," *Photonics*, vol. 9, no. 2, 2022, doi: 10.3390/PHOTONICS9020050.

Lyu, W., Xu, W., Yang, F., Chen, S., Tan, F., Yu, C., 2021. Non-invasive measurement for cardiac variations using a fiber optic sensor. IEEE Photon. Technol. Lett. 33 (18), 990–993. https://doi.org/10.1109/LPT.2021.3078757.

Min, R., Liu, Z., Pereira, L., Yang, C., Sui, Q.i., Marques, C., 2021. Optical fiber sensing for marine environment and marine structural health monitoring: a review. Opt. Laser Technol. 140, 107082.

Min, R., Hu, X., Pereira, L., Simone Soares, M., Silva, L.C.B., Wang, G., Martins, L., Qu, H., Antunes, P., Marques, C., Li, X., 2022. Polymer optical fiber for monitoring human physiological and body function: A comprehensive review on mechanisms, materials, and applications. Opt. Laser Technol. 147, 107626.

Mohamadou, Y., Kapen, P.T., Foutse, M., Kamga, A.L.K., Docna, O., Mohammad, M., Ahmad, M., Rabbani, K.-e., 2022. Design and development of a phonocardiograph for telemedicine applications. Health Technol. (Berl) 12 (2), 453–463.

Mokhtar, M.R., Sun, T., Grattan, K.T.V., 2012. Bragg grating packages with nonuniform dimensions for strain and temperature sensing. IEEE Sens. J. 12 (1), 139–144. https://doi.org/10.1109/JSEN.2011.2134845.

Moseley, S., Scaramuzza, N., Tasson, J.D., Trostel, M.L., 2019. Lorentz violation and Sagnac gyroscopes. Phys Rev D 100 (6). https://doi.org/10.1103/PHYSREVD.100.064031.

J. Nedoma et al., "Magnetic resonance imaging compatible non-invasive fibre-optic sensors based on the bragg gratings and interferometers in the application of monitoring heart and respiration rate of the human body: a comparative study," Sensors (Switzerland), vol. 18, no. 11, 2018, doi: 10.3390/s18113713.

J. Nedoma, M. Fajkus, R. Martinek, and H. Nazeran, "Vital sign monitoring and cardiac triggering at 1.5 tesla: A practical solution by an MR-ballistocardiography fiber-optic sensor," Sensors (Switzerland), vol. 19, no. 3, 2019, doi: 10.3390/S19030470.

Nedoma, J., Fajkus, M., Martinek, R., Vasinek, V., 2017. Non-invasive fiber-optic biomedical sensor for basic vital sign monitoring. Adv Electr Electron Eng 15 (2), 336–342. https://doi.org/10.15598/AEEE.V15I2.2131.

Niswar, M., Nur, M., Ilham, A.A., Mappangara, I., 2019. A low cost wearable medical device for vital signs monitoring in low-resource settings. Int. J. Electr. Comput. Eng. 9 (4), 2321–2327. https://doi.org/10.11591/IJECE.V9I4.PP2321-2327.

Osório, J.H., Guimarães, W.M., Peng, L.u., Franco, M.A.R., Warren-Smith, S.C., Ebendorff-Heidepriem, H., Cordeiro, C.M.B., 2021. Exposed-core fiber multimode interference sensor. Results in Optics 5, 100125.

Pereira, C.B., Kunczik, J., Bleich, A., Haeger, C., Kiessling, F., Thum, T., Tolba, R., Lindauer, U., Treue, S., Czaplik, M., 2019. Perspective review of optical imaging in welfare assessment in animal-based research. J. Biomed. Opt. 24 (07), 1.

C. Perezcampos Mayoral et al., "Fiber Optic Sensors for Vital Signs Monitoring. A Review of Its Practicality in the Health Field," Biosensors (Basel), vol. 11, no. 2, 2021, doi: 10.3390/BIOS11020058.

Perri, C., Arcadio, F., D'Agostino, G., Cennamo, N., Porto, G., Zeni, L., 2021. Chemical and biological applications based on plasmonic optical fiber sensors. IEEE Instrum. Meas. Mag. 24 (5), 50–55. https://doi.org/10.1109/MIM.2021.9491004.

Podbreznik, P., Đonlagić, D., Lešnik, D., Cigale, B., Zazula, D., 2013. Cost-efficient speckle interferometry with plastic optical fiber for unobtrusive monitoring of human vital signs. J. Biomed. Opt. 18 (10), 107001 https://doi.org/10.1117/1.JBO.18.10.107001.

"RAGE-12-Nalong health." https://www.aecg.com.cn/index.php?m=Alone&a=index&id=70 (accessed Feb. 01, 2023).

Rodríguez-Cuevas, A., Peña, E.R., Rodríguez-Cobo, L., Lomer, M., Higuera, J.M.L., 2017. Low-cost fiber specklegram sensor for noncontact continuous patient monitoring. J. Biomed. Opt. 22 (3), 037001 https://doi.org/10.1117/1.JBO.22.3.037001.
P. Samartkit, S. Pullteap, "Fiber optic sensor applications for vital signs monitoring: a review," iEECON 2019 – 7th International Electrical Engineering Congress, Proceedings, p. 1-4, 2019, doi: 10.1109/IEECON45304.2019.8938942.
Samartkit, P., Pullteap, S., Seat, H.C., 2021. Validation of fiber optic-based fabry-perot interferometer for simultaneous heart rate and pulse pressure measurements. IEEE Sens. J. 21 (5), 6195–6201. https://doi.org/10.1109/JSEN.2020.3041782.
Shono, A., Mori, S., Yatomi, A., Kamio, T., Sakai, J., Soga, F., Tanaka, H., Hirata, K.-I., 2019. Ultimate third heart sound. Intern. Med. 58 (17), 2535–2538.
Shoushan, M.M., Reyes, B.A., Rodriguez, A.M., Chong, J.W., 2021. Non-contact HR monitoring via smartphone and webcam during different respiratory maneuvers and body movements. IEEE J. Biomed. Health Inform. 25 (2), 602–612. https://doi.org/10.1109/JBHI.2020.2998399.
Stefani, A., Stecher, M., Town, G.E., Bang, O., 2012. Direct writing of fiber bragg grating in microstructured polymer optical fiber. IEEE Photon. Technol. Lett. 24 (13), pp. https://doi.org/10.1109/LPT.2012.2197194.
Suaste-Gómez, E., Hernàndez-Rivera, D., Sanchez-Sanchez, A.S., Villarreal-Calva, E., 2014. Electrically insulated sensing of respiratory rate and heartbeat using optical fibers. Sensors (Switzerland) 14 (11), 21523–21534. https://doi.org/10.3390/S141121523.
Sun, Q., Luo, H., Luo, H., Lai, M., Liu, D., Zhang, L., 2015. Multimode microfiber interferometer for dual-parameters sensing assisted by Fresnel reflection. Opt. Express 23 (10), 12777. https://doi.org/10.1364/OE.23.012777.
Suresh Kumar, V., Krishnamoorthi, C., 2021. Development of electrical transduction based wearable tactile sensors for human vital signs monitor: fundamentals, methodologies and applications. Sens. Actuators, A 321, 112582.
Tan, F., Chen, S., Lyu, W., Liu, Z., Yu, C., Lu, C., Tam, H., 2019. Non-invasive human vital signs monitoring based on twin-core optical fiber sensors. Biomed. Opt. Express 10 (11), 5940. https://doi.org/10.1364/BOE.10.005940.
Tan, F.Z., Lyu, W.M., Chen, S.Y., Liu, Z.Y., Yu, C.Y., 2020. Contactless vital signs monitoring based on few-mode and multi-core fibers. Opto-Electron Adv 3 (5), 1–12. https://doi.org/10.29026/OEA.2020.190034.
Y. Tang, J. Cang, Y. Yao, and C. Chen, "Displacement measurement of a concrete bridge under traffic loads with fibre-reinforced polymer-packaged optical fibre sensors," Adv. Mech. Eng., vol. 12, no. 3, 2020, doi: 10.1177/1687814020910538.
C. Tavares, C. Leitão, D. Lo Presti, M. Domingues, N. Alberto, H. Silva, and P. Antunes, "Respiratory and heart rate monitoring using an FBG 3D-printed wearable system," Biomed. Opt. Express., vol. 13, no. 4, p. 2299, 2022, doi: 10.1364/BOE.452115.
Teng, C., Min, R., Zheng, J., Deng, S., Li, M., Hou, L., Yuan, L., 2022. Intensity-modulated polymer optical fiber-based refractive index sensor: a review. Sensors 22 (1). https://doi.org/10.3390/S22010081.
Tian, K., Farrell, G., Wang, X., Yang, W., Xin, Y., Liang, H., Lewis, E., Wang, P., 2017. Strain sensor based on gourd-shaped single-mode-multimode-single-mode hybrid optical fibre structure. Opt. Express 25 (16), 18885–18896. https://doi.org/10.1364/OE.25.018885.
Tippit, H., Benchimol, A., 1967. The Apex Cardiogram. J. Am. Med. Assoc. 201 (7), 549. https://doi.org/10.1001/JAMA.1967.03130070069023.
Wang, K., Dong, X., Kohler, M., Kienle, P., Bian, Q., Jakobi, M., Koch, A., 2021. Advances in optical fiber sensors based on multimode interference (MMI): a review. IEEE Sens. J. 21 (1), 132–142. https://doi.org/10.1109/JSEN.2020.3015086.
Y. C. Wang, L. H. Shyu, and C. P. Chang, "The comparison of environmental effects on Michelson and Fabry-Perot interferometers utilized for the displacement measurement," Sensors, vol. 10, no. 4, 2010, doi: 10.3390/s100402577.
Z. Wang, G. Wang, Z. Wang, W. Gao, and Y. Cheng, "Incoherence suppression method of optical noises in a resonant fiber optic gyro based on the circularly polarized light propagation mechanism in a resonator," Opt Lett, vol. 46, no. 13, p. 3191, 2021, doi: 10.1364/OL.431065.
Y. Wang et al., "Noninvasive measurement of the vital signs of cancer patients with a dual-path microbend fiber sensor," Biomed Opt Express, vol. 13, no. 2, p. 982, 2022, doi: 10.1364/BOE.450258.
Wang, Y., Huang, Y., Bai, H., Wang, G., Hu, X., Kumar, S., Min, R., 2021. Biocompatible and biodegradable polymer optical fiber for biomedical application: a review. Biosensors (Basel) 11 (12). https://doi.org/10.3390/BIOS11120472.
Wang, Y.-L., Liu, B., Pang, Y.-N., Liu, J., Shi, J.-L., Wan, S.-P., He, X.-D., Yuan, J., Wu, Q., 2021. Low-cost wearable sensor based on a D-shaped plastic optical fiber for respiration monitoring. IEEE Trans. Instrum. Meas. 70, 1–8.
Wang, S., Ni, X., Li, L., Wang, J., Liu, Q., Yan, Z., Zhang, L., Sun, Q., 2020. Noninvasive monitoring of vital signs based on highly sensitive fiber optic mattress. IEEE Sens. J. 20 (11), 6182–6190. https://doi.org/10.1109/JSEN.2020.2974313.
Wang, F., Tanaka, M., Chonan, S., 2003. Development of a PVDF piezopolymer sensor for unconstrained in-sleep cardiorespiratory monitoring. J. Intell. Mater. Syst. Struct. 14 (3), 185–190. https://doi.org/10.1177/1045389X03014003006.
Wang, Q., Zhang, Y., Chen, G., Chen, Z., Hee, H.I., 2021. Assessment of heart rate and respiratory rate for perioperative infants based on ELC model. IEEE Sens. J. 21 (12), 13685–13694. https://doi.org/10.1109/JSEN.2021.3071882.
"World health statistics 2022: monitoring health for the SDGs, sustainable development goals." https://www.who.int/publications/i/item/9789240051157 (accessed 30, 2022).
Wu, S., Yin, S., Rajan, S., Yu, F.T.S., 1992. Multichannel sensing with fiber specklegrams. Appl. Opt. 31 (28), pp. https://doi.org/10.1364/ao.31.005975.
Xu, W., Shen, Y., Yu, C., Dong, B.o., Zhao, W., Wang, Y., 2020. Long modal interference in multimode fiber and its application in vital signs monitoring. Opt. Commun. 474, 126100.
Xu, W., Yu, C., Dong, B., Wang, Y., Zhao, W., 2022. Thin piezoelectric sheet assisted PGC demodulation of fiber-optic integrated MZI and its application in under mattress vital signs monitoring. IEEE Sens. J. 22 (3), 2151–2159. https://doi.org/10.1109/JSEN.2021.3128601.
Zawawi, M.A., O'Keffe, S., Lewis, E., 2013. Intensity-modulated fiber optic sensor for health monitoring applications: a comparative review. Sens. Rev. 33 (1), 57–67. https://doi.org/10.1108/02602281311294351.
Zaza, A., Ronchi, C., Malfatto, G., 2018. Arrhythmias and heart rate: Mechanisms and significance of a relationship. Arrhythm. Electrophysiol. Rev. 7 (4), 232–237. https://doi.org/10.15420/AER.2018.12.3.
X. Zhan, Y. Sun, F. Xiao, Y. Meng, J. Zhang, "Research on the Measurement of Heart Rate Based on LD Laser and Multimode Fiber," 2020 5th Optoelectronics Global Conference, OGC 2020, pp. 200–203, 2020, doi: 10.1109/OGC50007.2020.9260428.
Zhang, Y., Chen, Z., Hee, H.I., 2019. Noninvasive measurement of heart rate and respiratory rate for perioperative infants. J. Lightwave Technol. 37 (11), 2807–2814. https://doi.org/10.1109/JLT.2018.2883413.
Zhang, F., Yang, K., Pei, Z., Wu, Y., Sang, S., Zhang, Q., Jiao, H., 2022. A highly accurate flexible sensor system for human blood pressure and heart rate monitoring based on graphene/sponge. RSC Adv. 12 (4), 2391–2398. https://doi.org/10.1039/D1RA08608A.
Zhao, R., Du, L., Zhao, Z., Chen, X., Sun, J., Man, Z., Cao, B., Fang, Z., 2021. Accurate estimation of heart and respiration rates based on an optical fiber sensor using adaptive regulations and statistical classifications spectrum analysis. Front Digit Health 3. https://doi.org/10.3389/FDGTH.2021.747460.
Zhu, L., Kan, C., Du, Y., Du, D., 2019. Heart rate monitoring during physical exercise from photoplethysmography using neural network. IEEE Sens Lett 3 (1), 1–4.
Zhu, T., Wu, D., Liu, M., Duan, D.W., 2012. In-line fiber optic interferometric sensors in single-mode fibers. Sensors 12 (8), 10430–10449. https://doi.org/10.3390/S120810430.